NASA/TM—2014–218191

Wide Field X-Ray Telescope Mission Concept Study Results

R.C. Hopkins and H.D. Thomas
Marshall Space Flight Center, Huntsville, Alabama

L.L Fabisinski
ISSI, Jacobs ESSSA Group, Marshall Space Flight Center, Huntsville, Alabama

M. Baysinger, L.S. Hornsby, C.D. Maples, and T.E. Purlee
Jacobs ESSSA Group, Marshall Space Flight Center, Huntsville, Alabama

P.D. Capizzo
Raytheon, Jacobs ESSSA Group, Marshall Space Flight Center, Huntsville, Alabama

T.K. Percy
SAIC, Jacobs ESSSA Group, Marshall Space Flight Center, Huntsville, Alabama

March 2014

The NASA STI Program…in Profile

Since its founding, NASA has been dedicated to the advancement of aeronautics and space science. The NASA Scientific and Technical Information (STI) Program Office plays a key part in helping NASA maintain this important role.

The NASA STI Program Office is operated by Langley Research Center, the lead center for NASA's scientific and technical information. The NASA STI Program Office provides access to the NASA STI Database, the largest collection of aeronautical and space science STI in the world. The Program Office is also NASA's institutional mechanism for disseminating the results of its research and development activities. These results are published by NASA in the NASA STI Report Series, which includes the following report types:

- TECHNICAL PUBLICATION. Reports of completed research or a major significant phase of research that present the results of NASA programs and include extensive data or theoretical analysis. Includes compilations of significant scientific and technical data and information deemed to be of continuing reference value. NASA's counterpart of peer-reviewed formal professional papers but has less stringent limitations on manuscript length and extent of graphic presentations.

- TECHNICAL MEMORANDUM. Scientific and technical findings that are preliminary or of specialized interest, e.g., quick release reports, working papers, and bibliographies that contain minimal annotation. Does not contain extensive analysis.

- CONTRACTOR REPORT. Scientific and technical findings by NASA-sponsored contractors and grantees.

- CONFERENCE PUBLICATION. Collected papers from scientific and technical conferences, symposia, seminars, or other meetings sponsored or cosponsored by NASA.

- SPECIAL PUBLICATION. Scientific, technical, or historical information from NASA programs, projects, and mission, often concerned with subjects having substantial public interest.

- TECHNICAL TRANSLATION. English-language translations of foreign scientific and technical material pertinent to NASA's mission.

Specialized services that complement the STI Program Office's diverse offerings include creating custom thesauri, building customized databases, organizing and publishing research results…even providing videos.

For more information about the NASA STI Program Office, see the following:

- Access the NASA STI program home page at <http://www.sti.nasa.gov>

- E-mail your question via the Internet to <help@sti.nasa.gov>

- Phone the NASA STI Help Desk at 757–864–9658

- Write to:
  NASA STI Information Desk
  Mail Stop 148
  NASA Langley Research Center
  Hampton, VA 23681–2199, USA

NASA/TM—2014–218191

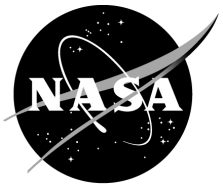

Wide Field X-Ray Telescope Mission Concept Study Results

R.C. Hopkins and H.D. Thomas
Marshall Space Flight Center, Huntsville, Alabama

L.L Fabisinski
ISSI, Jacobs ESSSA Group, Marshall Space Flight Center, Huntsville, Alabama

M. Baysinger, L.S. Hornsby, C.D. Maples, and T.E. Purlee
Jacobs ESSSA Group, Marshall Space Flight Center, Huntsville, Alabama

P.D. Capizzo
Raytheon, Jacobs ESSSA Group, Marshall Space Flight Center, Huntsville, Alabama

T.K. Percy
SAIC, Jacobs ESSSA Group, Marshall Space Flight Center, Huntsville, Alabama

National Aeronautics and
Space Administration

Marshall Space Flight Center • Huntsville, Alabama 35812

March 2014

TRADEMARKS

Available from:

NASA STI Information Desk
Mail Stop 148
NASA Langley Research Center
Hampton, VA 23681–2199, USA
757–864–9658

This report is also available in electronic form at
<http://www.sti.nasa.gov>

TABLE OF CONTENTS

LIST OF FIGURES

LIST OF FIGURES (Continued)

LIST OF TABLES

LIST OF TABLES (Continued)

LIST OF ABBREVIATIONS, ACRONYMS, AND SYMBOLS

ACS	attitude control system
AGN	active galactic nuclei
AOP	argument of perigee
AXTAR	Advanced X-ray Timing Array
CCD	charge-coupled device
C&DH	command and data handling
DAU	data acquisition unit
DPA	digital processing assembly
FEM	finite element model
FEMAP	finite element mapping and postprocessing
FMA	flight mirror assembly
HAST	High Accuracy Star Tracker
HEO	highly elliptical orbit
GN&C	guidance, navigation, and control
GR&A	ground rules and assumptions
KSC	Kennedy Space Center
LEO	low Earth orbit
LSP	Launch Services Program
LVA	launch vehicle adapter
MEL	master equipment list

LIST OF ABBREVIATIONS, ACRONYMS, AND SYMBOLS (Continued)

MLI	multilayer insulation
MRL	Manufacturing Readiness Level
MSFC	Marshall Space Flight Center
RCS	reaction control system
$R\&D^3$	Research and Development Degree of Difficulty
SE-L2	second Sun-Earth Lagrange point
STK	Systems Tool Kit
SWRI	Southwest Research Institute
TM	Technical Memorandum
TRL	Technology Readiness Level
UFSS	ultrafine Sun sensor
WFXT	Wide Field X-ray Telescope
ε^*	effective emissivity

TECHNICAL MEMORANDUM

WIDE FIELD X-RAY TELESCOPE MISSION CONCEPT STUDY RESULTS

1. INTRODUCTION

During the summer of 2012, the Advanced Concepts Office at the NASA George C. Marshall Space Flight Center (MSFC) completed a mission concept study for the Wide Field X-ray Telescope (WFXT) science team. The goal of the concept study was to complete a spacecraft conceptual design and investigate the feasibility of the proposed astrophysics mission, which is a near-all sky survey observing active galactic nuclei (AGN) and clusters of galaxies in order to further understand the structure and evolution of the universe.[1]

This Technical Memorandum (TM) includes a brief introduction to the science mission, a description of the requirements, spacecraft design, and mission concept, and risk and technology gap analyses that were completed during the study.

2. SCIENCE MISSION SUMMARY

A brief description of the WFXT science mission is presented here to provide some science background and justification for the design study. For a more detailed science mission discussion, the reader is referred to other publications authored by various members of the science team that detail the science mission.[2]

WFXT is an x-ray astrophysics survey mission that will probe the large-scale structure of the universe. From its highly elliptical orbit (HEO) about Earth, WFXT will use its three identical x-ray telescopes to complete wide, medium, and deep field surveys of the sky. The wide field survey will cover most of the extragalactic sky with higher sensitivity and better resolution than the ROSAT All Sky Survey; the medium field survey will map several thousand square degrees of the sky to the same sensitivity as Chandra; and the deep field survey will cover about 100 square degrees (or about 1,000 times) the area covered by the Chandra deep fields. The increased sensitivity and coverage of WFXT is provided by the x-ray optics that, while of comparable resolution to Chandra, offer a much wider high resolution field-of-view. In summary, WFXT will be orders of magnitude more effective than previous or planned x-ray missions in carrying out sky surveys.

The scientific benefits of x-ray sky surveys were recognized in the National Research Council's 2010 Decadal Survey, *New Worlds, New Horizons in Astronomy and Astrophysics*.[3] By observing the high-redshift objects near the edge of the known universe, WFXT will be able to probe far back in time, back to the era of galaxy and cluster formation. The science team anticipates that WFXT will detect essentially all extended x-ray sources associated with massive virialized clusters with a redshift (z) less than about 2, as well as large numbers of AGN. Some AGN will likely offer insight into the formation of black holes at the very beginning of the galaxy formation era. Data collected by WFXT will provide valuable insight into galaxy and galactic cluster formation, the large-scale structure of the universe, black hole evolution, and the interaction of gravity, dark matter, and dark energy.

3. SCIENCE INSTRUMENTS AND OPERATION

The description of the instruments presented below is to the level required for the concept study and is not a detailed description of all components of the instruments and their operation. The data included here are the data that were considered relevant to the spacecraft design, such as instrument operating power, thermal requirements, mass, and similar parameters.

Tables 1 and 2 provide a top-level summary of the instrument data and were provided by the science team. Additional thermal requirements and assumptions are included in section 7.7 of this TM. Regarding the data storage and download rates, since this is a survey mission that is counting photons and not taking pictures of the sky, the amount of data collected during an observing session is fairly small. The storage and download requirements were provided by the science team, who had estimated these values based on detector parameters and expected activity. The spacecraft design team used these values as given.

Table 1. Basic science instrument dimensions and requirements.

Instrument Mass and Power/Thermal Requirements (Provided by Principal Investigator)				
Instruments	Size (mm)	Mass (kg)	Power (W)	Temperature (°C)
X-ray telescope	1,200 dia. × 500 len.	300	100	20
Optical bench	shape = cone, len = 5,000, dia_front = 1,200, dia_rear = 500	75	–	–
CCD focal plane assembly	250 × 150 × 200	25	4	–90
Digital electronics assembly	230 × 180 × 230	4	12	–
Aspect camera and fiducial light system	–	20	25	–
Total per instrument (without contingency)	–	424	141	–
Total for 3 telescope assemblies	–	1,272	423	–
Digital processing assembly	230 × 180 × 180	6	20	–
Total for all instruments	–	1,278	443	–

Table 2. Instrument data and download rates.

Instrument Data and Download Rates (Provided by Principal Investigator)	
Storage	128 Gbits
Download rate	128 kbps
Download frequency	Daily (desired)

During observations, WFXT will maintain an inertially fixed attitude for a certain amount of time and collect data before slewing to another part of the sky. Each observation period can vary from 2 to 100,000 s, although the observation time does not have to be continuous, but can allow breaks for spacecraft functions, eclipse periods, and similar events. Another observing mode that may or may not be implemented involves the observatory slowly rocking back and forth as it sweeps across the sky, essentially observing the sky in a strip before moving on to another part of the sky and generating another strip of observations. The spacecraft team designed the pointing control system to meet the requirements of the pointed observation mode. Because detailed requirements for the sweeping mode were not finalized, this mode was not considered during the spacecraft design session.

Daily downloads of data are preferred, but not critical since WFXT is not looking for targets of opportunity (as do some observatories such as Fermi). This download frequency is very modest, and should pose no problems as Chandra, a similar astrophysics mission in a similar orbit, downloads daily.

4. STUDY APPROACH

The study was actually completed in two sessions. The first session was a quick design, with the goal being to test the feasibility of the mission. The second phase was primarly focused on trades that could improve the design, reduce cost and complexity, and to complete a risk analysis and technology gap assessment for both the spacecraft and the science instruments. The results presented in this TM are the culmination of both design sessions.

The design team's approach for this concept study was to consider the spacecraft bus as a custom design. Justification included the fact that even an off-the-shelf bus will probably need modification given the unusual payload configuration, and estimating the cost of modifying an existing bus is difficult and best done by the bus manufacturer or by the Rapid Spacecraft Development Office at Goddard Space Flight Center. Since those types of cost estimates typically take more time than was allotted for the design study, the team created a custom bus design and used that for the cost estimate. Also, considering the design maturity of the instruments, the team placed a 30% mass and power margin on the instruments, along with the same mass and power margin for the spacecraft bus.

5. MISSION AND SPACECRAFT REQUIREMENTS

The three possible orbits being considered for WFXT are illustrated in figure 1, and include low Earth orbit (LEO) (about 600 km altitude, circular, and nearly equatorial); a Chandra-type, HEO with perigee and apogee altitudes of 16,000 and 133,000 km, respectively; and a halo orbit about the second Sun-Earth Lagrange point (SE-L2). Each has its advantages and disadvantages, but given the experience that the science team has with Chandra, the Chandra-type orbit was selected as the baseline orbit. The appeal of the LEO option is mainly to allow the use of a smaller (and less expensive) launch vehicle, although the impacts to science are not clearly known at this point. The SE-L2 halo orbit would allow the least restricted science observations and the most stable thermal environment, but could prove more costly by requiring a higher launch energy, more complex orbit maintenance, and higher power for communications. As a brief, top-level exercise, the design team also assessed the possible impact that operating in LEO would have on the spacecraft subsystems, the results of which are presented in section 10.

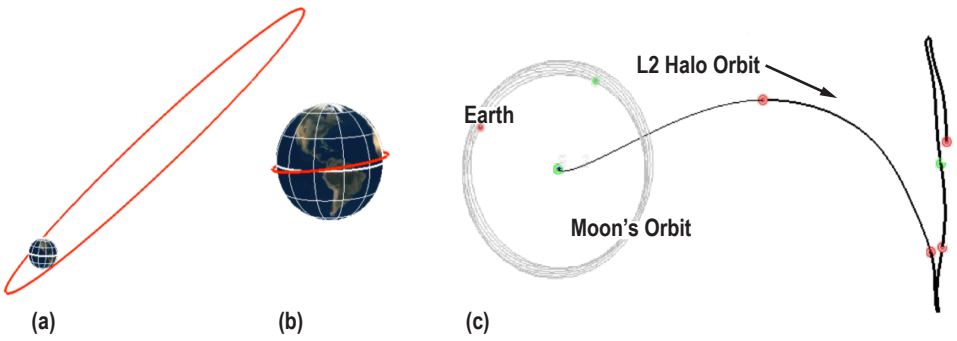

Figure 1. Possible orbits for WFXT: (a) An orbit similar to Chandra, (b) LEO, and (c) a halo orbit about the SE-L2 point. For this concept study, the Chandra-type orbit was selected.

An additional constraint placed on the observatory is a 45-deg Sun avoidance angle, which is the included angle measured between the boresight of the coaligned telescopes and a line connecting the observatory to the Sun. This avoidance angle is necessary to prevent sunlight from directly entering the x-ray telescopes and impacting the charge-coupled device (CCD) detectors at the rear of the optical benches. The x-ray telescopes themselves would be unaffected, but the CCD detectors would be damaged.

Working with the customer and determining the mission and spacecraft performance requirements is a top priority before the design study begins. After several iterations with the science team to make sure that the requirements were understood, the study leads provided the design team with the requirements listed in table 3.

Table 3. Mission and spacecraft requirements for the design study.

Requirement	Value		
Launch year	2020		
Mission duration	3 (5) yr, with possible extension to 10 yr		
Orbit	Chandra-type HEO (16,000 × 133,000 km altitude)		
Launch vehicle	No particular vehicle selected		
Payload description	3 x-ray telescopes, coaligned within 1 arcmin (or better)		
Payload power (total, without contingency)	443 W		
Payload mass (total, without contingency)	1,278 kg		
Data downlink	128 kbps		
Data storage	128 Gbits		
Pointing	3-axis stabilized (roll defined as along the boresight of the instrument)		
Accuracy (pitch, yaw, roll)	30 arcsec	30 arcsec	1 deg
Knowledge (pitch, yaw, roll)	2 arcsec	2 arcsec	30 arcsec
Stability (pitch, yaw, roll)	0.8 arcsec per 1/3 s	0.8 arcsec per 1/3 s	30 arcsec per 1/3 s
Rapid slew requirements	120 deg in 10 min if in LEO (Note: LEO is not the baseline orbit, but an option)		
Slow slew requirements	1 arcsec for scanning mode (if used; it is not the baseline observing method)		
Repointing slew requirements	1 deg/min; 3 per day (for spacecraft operations; not driven by science)		
Sun avoidance angle	45 deg		
Other avoidance angles	Moon and Earth limb, 10–15 deg		
Duration of each pointed observation	2–100,000 s (does not have to be contiguous)		

6. MISSION ANALYSIS

Mission analysis for this study included determining launch vehicle performance and using Systems Tool Kit (STK) to calculate ground contact durations, beta angle history, eclipse durations, and orbital element variations during the mission lifetime.

Table 4 lists the official performance data provided by NASA Launch Services Program (LSP). The two possible ascent profiles—2-burn and 3-burn—offer slightly different performance. With the 3-burn profile, the launch vehicle upper stage pauses in a circular orbit before initiating the transfer to the target orbit. The 2-burn profile, however, does not use the parking orbit, placing the upper stage on a direct transfer to the target orbit. While the performance of the 2-burn profile is slightly better, that type of ascent does not allow mission planners much flexibility in targeting different values of argument of perigee (AOP). Being able to select the AOP allows mission planners to minimize eclipse times during the mission. The 3-burn profile, while resulting in less performance, allows planners to target any AOP since the launch vehicle parks in a circular orbit before maneuvering to the final orbit. The study team recommends using the 3-burn profile for the WFXT mission due to the flexibility it offers in targeting various AOP values.

Table 4. Launch vehicle performance estimates provided by NASA Launch Services Program.

Launch Vehicle	Ascent Profile	Payload as Quoted by LSP	Payload with 15% Launch Vehicle Reserve
Atlas V 521	2-burn	3,355	2,850
Atlas V 531	2-burn	3,995	3,395
Atlas V 521	3-burn	3,305	2,805
Atlas V 531	3-burn	3,950	3,355

The analysis team used STK to propagate orbits for various start times. The initial orbit is 16,000×133,000 km at an inclination of 28.5 deg. In order to compare the results for different launch times and to reduce the number of varied parameters to just one (i.e., start time), an Earth-fixed beginning Cartesian state was approximated for a launch from Kennedy Space Center (KSC).

First, the simple ascent launch vehicle model was used to obtain the flight path from KSC to a point that matches the latitude and longitude of MECO2 on a Atlas V 521 3-burn geosynchronous orbit mission. The orbit at this point is assumed to be 185×133,000 km, and the time from liftoff is 27 min.

The orbit is then propagated (using the High-Precision Orbit Propagator) from 185 to 133,000 km. The transfer time is 27.25 hr. The Centaur is then used to raise the perigee from 185 to 16,000 km, resulting in the desired mission orbit. The Earth-fixed state at this point, along with the Earth-to-orbit path, is shown in figure 2.

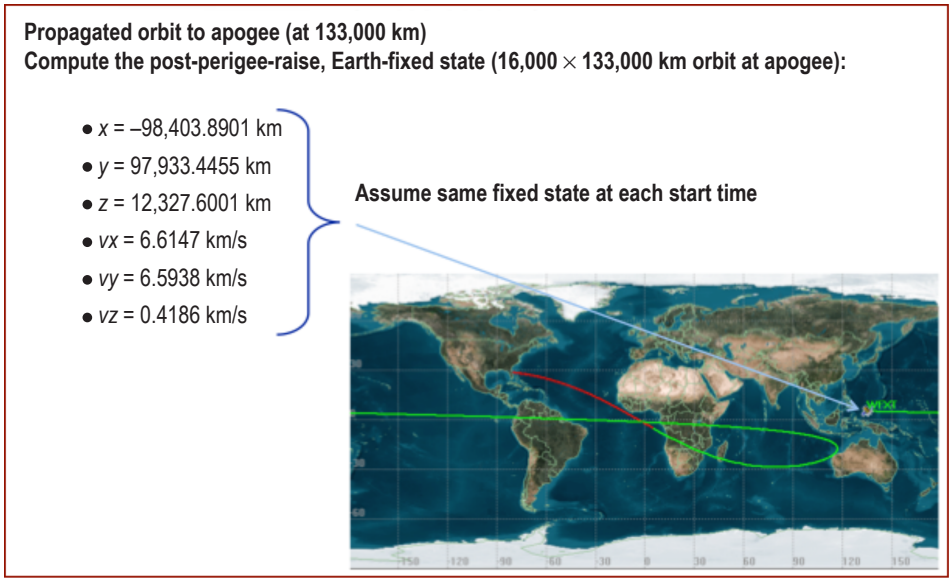

Figure 2. Summary of method used to determine initial state for beta angle and eclipse duration histories.

Results for the beta angle history are plotted in figure 3. For each start time, the corresponding beta angle is plotted over the 5-yr mission time. The January through June launch date cases are shown in figure 3(a), while figure 3(b) plots the July through December launch date cases. Maximum beta angle magnitudes for the separate launch dates range from about 9 to 51 deg.

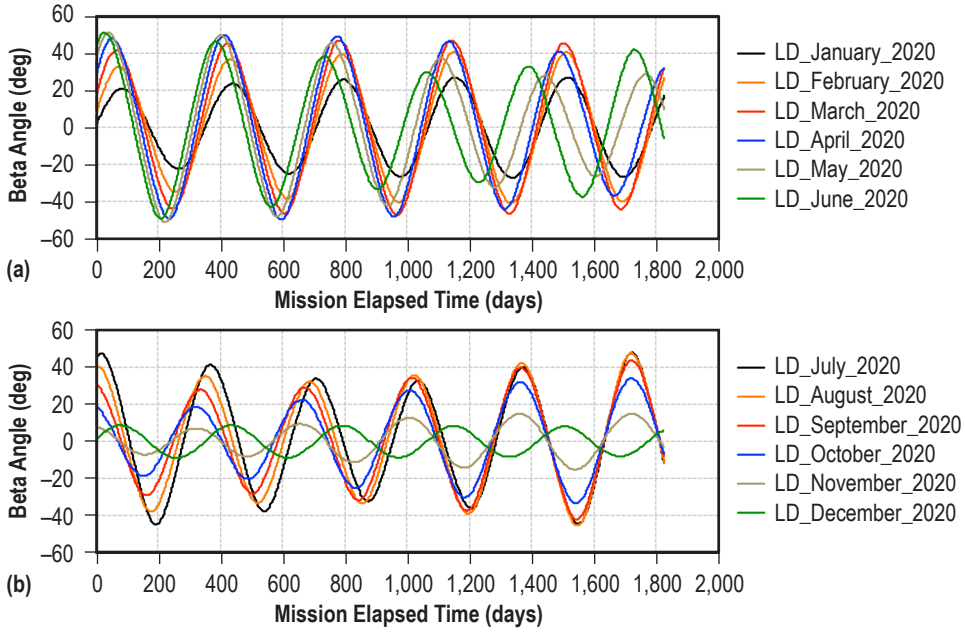

Figure 3. Beta angle histories for various orbit insertion dates: (a) January through June 2020 and (b) July through December 2020.

Figure 4 shows the maximum eclipse durations that occur for the different launch dates. The maximum is 274 min (December launch), and the minimum is 170.3 min (August launch). The eclipses during the 5-yr mission are mostly due to Earth with occasional lunar eclipses.

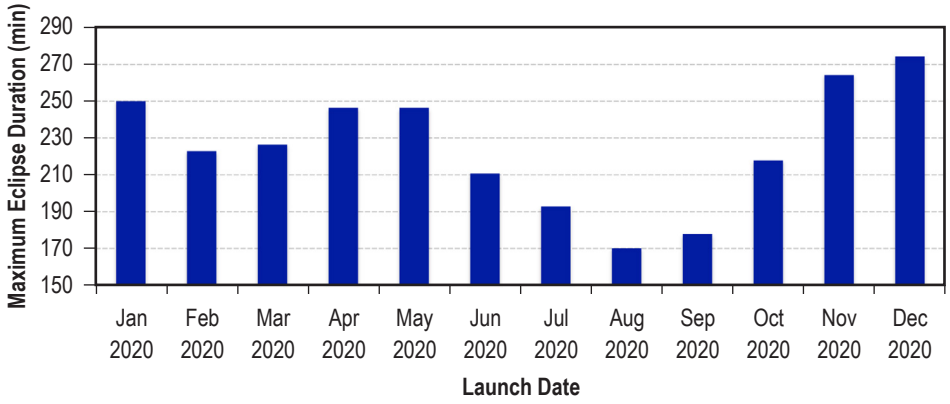

Figure 4. Eclipse duration history.

The launch date with the lowest maximum eclipse duration is the August 1 case with a maximum eclipse duration of 170.3 min and a maximum beta angle magnitude of 47.7 deg. More cases should be run around this launch date to converge on a refined minimum case and to also show the local sensitivity to launch date (possibly leading to a launch window to stay below a desired eclipse number).

Depending on the initial orbit orientation, the inclination may vary by small or large amounts. Chandra, for example, which began in a similar orbit with an inclination around 28.5 deg, is now at an inclination of over 70 deg. However, no constraints were given on inclination, so this drift in inclination is acceptable and does not require any orbit maintenance. Inclination drift for various launch dates (which determine initial orbit orientation) is plotted in figure 5.

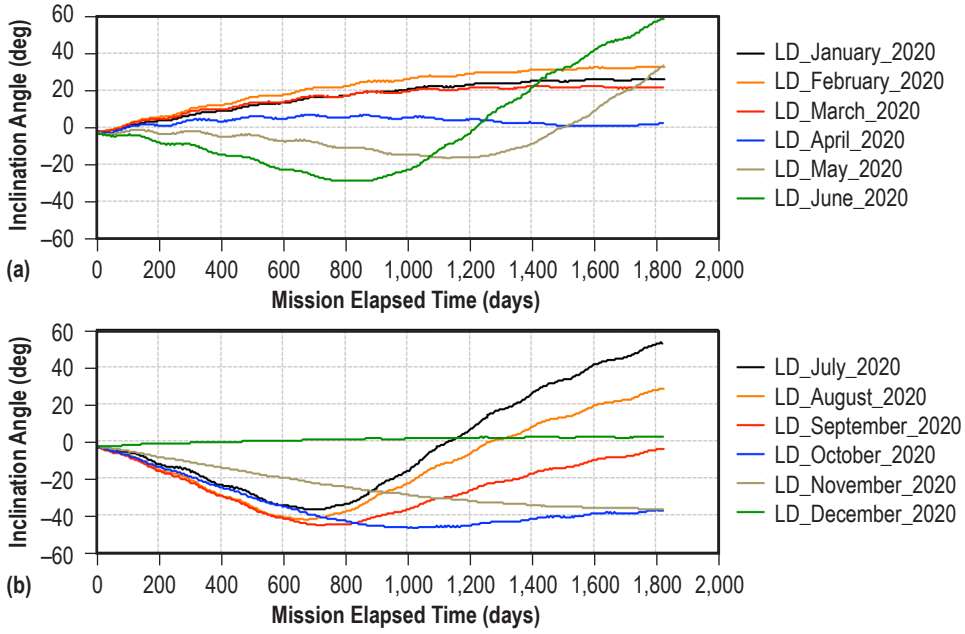

Figure 5. Variation of orbit inclination for various launch dates: (a) January through June 2020 and (b) July through December 2020.

In addition to inclination changes, orbit perturbations due to Earth's oblateness, the Moon, Sun, and other bodies cause the perigee and apogee to change over time as well. These variations are plotted in figures 6 and 7. The perigee altitude decreases dramatically in some cases, with a minimum of approximately 2,850 km for a June launch. This is still well outside the atmosphere and should not cause any problems.

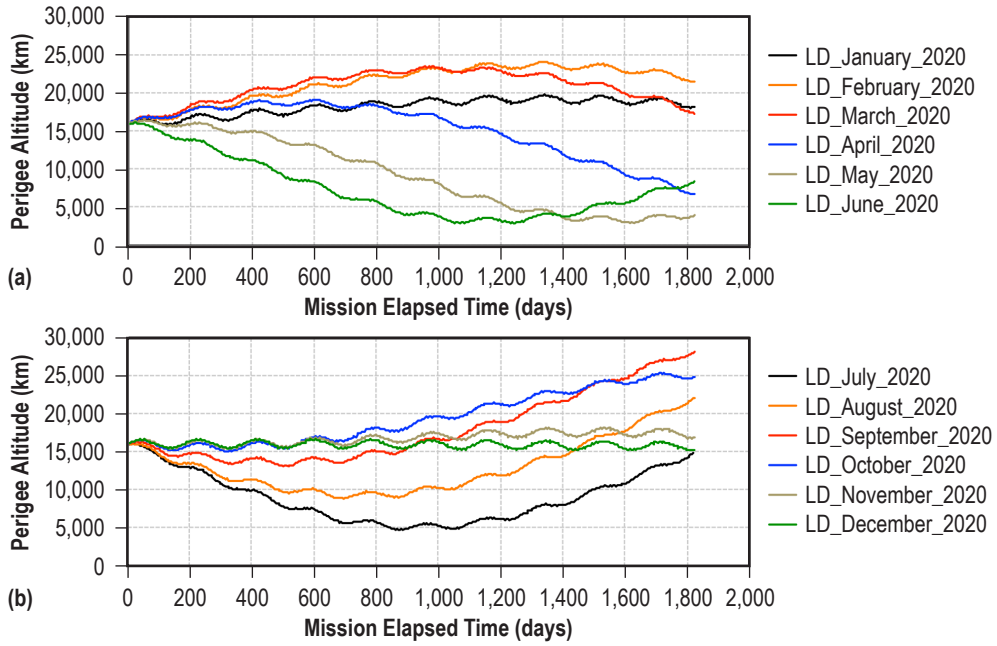

Figure 6. Variations in perigee over time for various launch dates: (a) January through June 2020 and (b) July through December 2020.

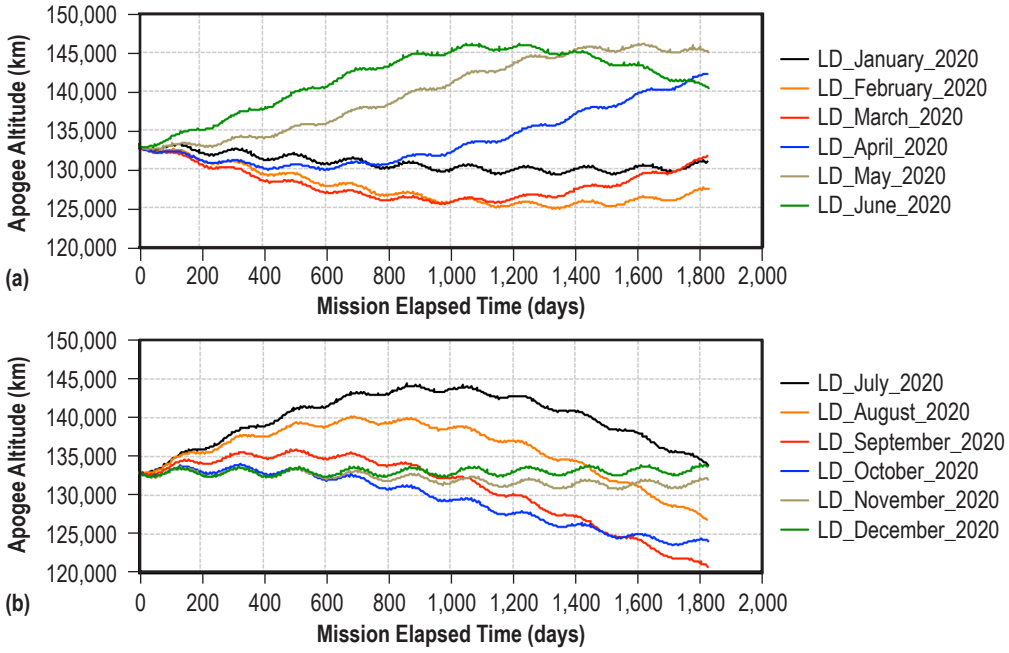

Figure 7. Variations in apogee over time for various launch dates: (a) January through June 2020 and (b) July through December 2020.

7. SPACECRAFT DESIGN

Details for the spacecraft design are presented below, and include descriptions of the overall configuration as well as subsystems. Each subsystem section contains a description of ground rules and assumptions (GR&A) used to guide the design, approach, and methodology, and a master equipment list (MEL) showing the components selected for this conceptual design.

Overall, the bus uses typical components with none of the subsystem elements requiring technological development. All requirements as listed in table 1 are met with the proposed design. It should be noted that the bus is not completely optimized (due to study duration limitations) and is not the only valid design approach. It does, however, accomplish the primary goal of checking the feasibility and cost of the WFXT mission as proposed.

7.1 Configuration

The WFXT study spacecraft was broken down into two separate major pieces. The telescopes were considered to be provided by the science team, and no changes were made. The spacecraft was designed to meet the science requirements of the telescopes and to the other requirements of the mission. The basic configuration for the observatory is shown in figure 8. The science telescopes were placed radially around the centerline to minimize size. The spacecraft bus was then designed around the telescopes to be large enough to provide space for the supporting systems and to fit within a 4-m launch vehicle shroud. A hexagonal shape was chosen for the bus, and the spacecraft systems are mostly mounted on the inner walls. The diameter of the hexagonal bus was also sized to mate to an Atlas Truss adapter. This allows for a minimal, nonstructural telescope door. The telescope door serves as both a sunshade and also a protective covering. The pair of solar arrays both fold and stow against the side of the spacecraft bus. The arrays are sized so the single panel size is approximately the size of the spacecraft bus panel.

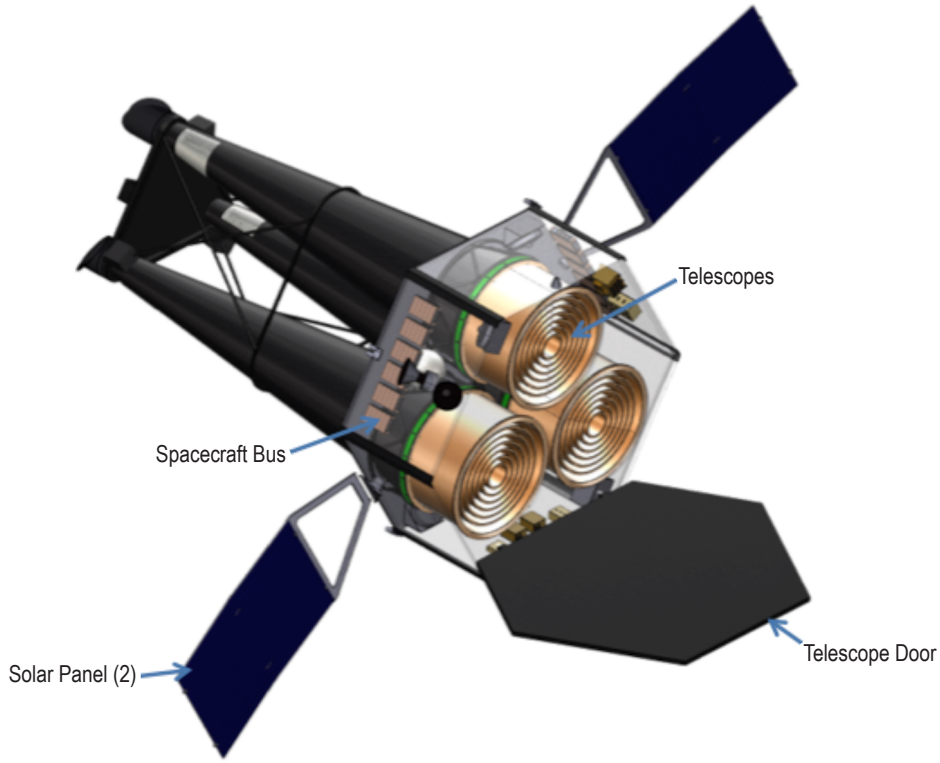

Figure 8. The WFXT Observatory configuration showing the science instruments and major spacecraft bus components.

Basic dimensions are shown in figure 9. The total size of the spacecraft is 6 m tall by 3.7 m in diameter. This size allows for the spacecraft to fit within a typical 4-m-diameter launch shroud.

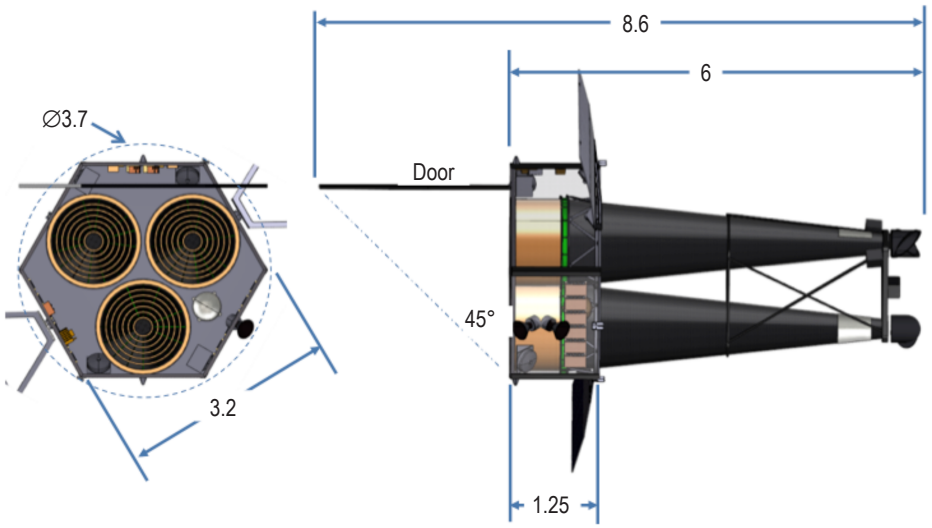

Figure 9. Basic dimensions of the observatory (all dimensions in meters).

7.2 Mass Properties

The WFXT mass rollup is listed in table 5. The WFXT study basic dry mass total is 716 kg when the following subsystem masses are rolled up: structures, propulsion, thermal, avionics, and power. This increases to 931 kg of predicted mass after adding a 30% contingency of 214 kg. The predicted dry mass consists of the basic dry mass and the contingency added by each subsystem, which is 30% (214 kg); this increases the dry mass total to 931 kg.

Table 5. Master equipment list.

WFXT			Basic Mass (kg)	Contingency (%)	Contingency (kg)	Predicted Mass (kg)
1.0	Structures		384.36	30	115.31	499.67
2.0	Propulsion		15.44	30	4.63	20.07
3.0	Thermal		27	30	8.1	35.1
4.0	Avionics		161.86	30	48.56	210.42
5.0	Power		127.6	30	38.28	165.88
Dry Mass			716.26	30	214.88	931.14
6.0	Nonpropellant fluids		0.12	0	0	0.12
7.0	Payload		1,278	30	383.4	1,661.4
Inert mass			1,278.12			1,661.52
Total less propellant			1,994.38			2,592.66
8.0	Propellant		32.33			32.33
	8.1	Hydrazine	32.33			32.33
Vehicle mass			2,026.71			2,624.99
Launch vehicle adapter (LVA) (T3302)			181.4			181.4
Total vehicle mass including LVA			2,208.11			2,806.39

Adding nonpropellant fluids and the payload to the dry mass totals to the inert mass. The basic inert mass for the WFXT study is 1,278 kg, and the predicted inert mass is 1,662 kg after adding in the 30% contingency of 383 kg on the payload. Adding 32 kg of propellant (hydrazine) to the dry mass and inert mass (total less propellant) gives a vehicle basic mass of 2,027 kg and a vehicle predicted mass of 2,625 kg.

The launch vehicle adapter (LVA) selected is the T3302, which weighs 181 kg maximum. This results in a total basic vehicle mass including LVA of 2,208 kg and a total predicted vehicle mass including LVA of 2,806 kg.

The Technology Readiness Level (TRL) analysis for this vehicle resulted in an average of 8.7 per component due to the high number of TRL 9 components.

7.3 Propulsion

The WFXT propulsion system is responsible only for momentum unloading (see table 6). A monoprop blowdown system is designed using the same engine and tank as the Chandra spacecraft as well as other available flight-proven components (see fig. 10). The fuel is hydrazine, and the pressurant is gaseous nitrogen. The system consists of eight NGST MRE-0.1 thrusters and a single ATK 80384-1 diaphragm tank. The tank holds the required 26 kg of propellant for momentum unloading plus about 6 kg extra. The total propellant load including residuals is 32.3 kg, and the nitrogen mass is 0.12 kg. Along with the dry masses listed in table 7, the total propulsion system wet mass is 53 kg.

Table 6. Propulsion GR&A.

Category	Value
Responsibilities	Momentum unloading
System type	Monopropellant blowdown
Fuel	Hydrazine
Pressurant	Gaseous nitrogen
Engine	NGST MRE-0.1 Thrust = 0.2 lbf *Isp* = 216 s

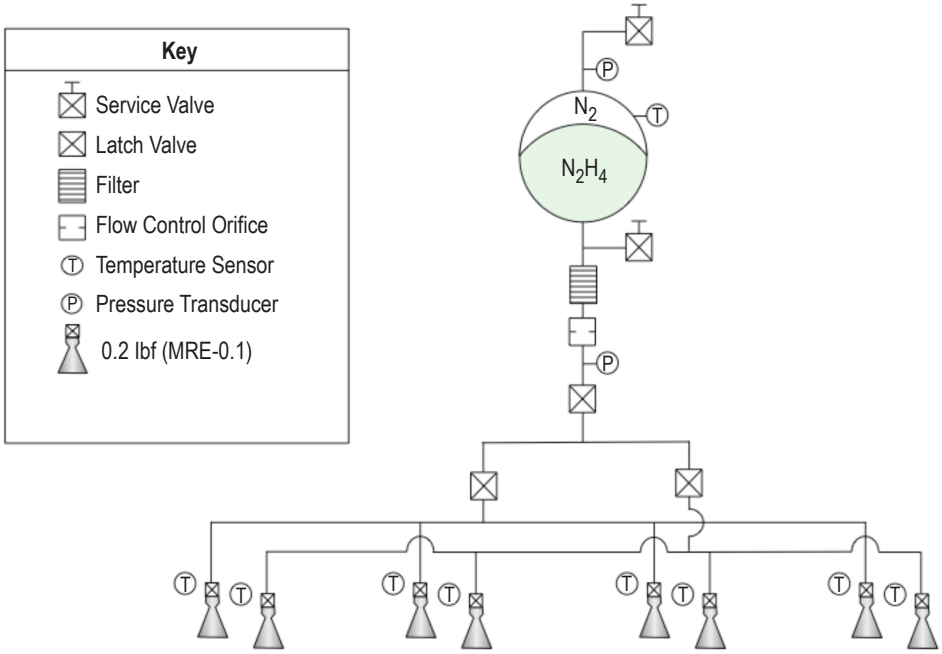

Figure 10. The spacecraft concept uses a simple monoprop system with Chandra heritage.

Table 7. Propulsion system MEL.

Item	Quantity	Unit Mass (kg)	Basic Mass (kg)	Contingency		Predicted Mass (kg)	Information
				(%)	(kg)		
Propulsion total			15.44	30	4.6	20.07	
Thrusters (0.2 lbf engines)	8	0.5	4	30	1.2	5.2	NGST MRE-0.1
Propellant tanks	1	5.9	5.9	30	1.77	7.67	ATK (80384-1)
Pressurant fill/drain valve	1	0.21	0.21	30	0.06	0.27	Moog (50E889)
Pressure transducers	2	0.28	0.56	30	0.17	0.73	Lunar Prospector
Propellant filters	1	0.3	0.3	30	0.09	0.39	VACCO (F1D10559-01)
Venturi	1	0.02	0.02	30	0.01	0.03	AIAA 2003-4470
Latch valves	3	0.36	1.08	30	0.32	1.4	Moog (51-166)
Propellant fill/drain valves	1	0.21	0.21	30	0.06	0.27	Moog (50-787)
Lines and fittings	1	2.08	2.08	30	0.62	2.7	Estimate
Structural mounts	1	1.08	1.08	30	0.32	1.4	Estimate

7.4 Avionics

Avionics includes command and data handling (C&DH), communications, as well as guidance, navigation, and control (GN&C). The GR&A that guided the avionics subsystem design is listed in table 8.

Table 8. Avionics subsystem GR&A.

Category	Value
C&DH	Spacecraft bus will perform avionic functions, including thermal control and power switching for the science payload. The payload will perform data collection and processing, including analog-to-digital conversion and any data compression required. The spacecraft bus will provide data storage required for downlink.
Total science downlink communication data rate	128 kbps continuous data collection rate
Daily download frequency	Once every 24 hr, desired but not required
Total science onboard memory required	Up to 24 hr of data to be stored onboard, 11 Gbits minimum, 128 Gbits desired
Fault tolerance	Single fault tolerance for critical systems—mission success
Pointing control	3-axis stabilized, zero momentum biased
Operational pointing scenarios/viewing coverage	3-axis stabilized pointing anywhere in field of regard. Possible slow scanning mode over small bands. May have paired targets to avoid occultation loss times. (No roll allowed for thermal or power management during observation periods, 28 hr minimum.)
Duration of pointing observations	Up to 100,000 s (28 hr) accumulated total time. 28 hr continuous desired; interrupts for Sun avoidance are acceptable.
Slow slew requirements (scanning)	2.7 arcsec/s for scanning mode (2.7 deg/hr) for a duration of 20,000 to 40,000 s (5.5 to 11 hr). 1–2 arcsec knowledge at a rate of 3 Hz
Fast slew requirements (avoidance and repointing slew requirements)	12 deg/min (60 deg in 10 min), 1 time per orbit minimum
Sun avoidance angle	Up to 60 deg Sun avoidance maneuvers are to be performed whenever required.
Other avoidance angles	No avoidance maneuvers required for Earth and Moon.
Accuracy (pitch, yaw, roll)	30 arcsec pitch and yaw, 1 deg roll
Knowledge (pitch, yaw, roll)	2 arcsec pitch and yaw, 30 arcsec roll
Stability (pitch, yaw, roll)	0.8 arcsec per 1/3 s pitch and yaw, 30 arcsec per 1/3 s roll
Reaction wheel desaturation	RCS will be used for reaction wheel desaturation.

7.4.1 Command and Data Handling

The spacecraft bus will perform avionics functions including thermal control and power switching for the science instruments, data storage, and downlink operations. The science payload will perform data processing including analog-to-digital conversion and data compression and filtering. The downlink frequency required is at least once in a 24-hr period. Chandra downlinked once every 8 hr, probably for operational purposes. The total science data collection rate is 128 kbps. This is assumed a continuous rate during science observations. The desired total science onboard memory is 128 Gbits. Single fault tolerance is used for critical systems and mission success. Most avionics systems are considered critical, where bus instrumentation can be single string. A robust avionics attitude control system (ACS) is desired to prevent Sun damage.

An avionics trade was performed on general-purpose flight computers able to perform thermal and power management, and provide data storage and downlink functions. Option 1, the Saab Ericsson Space computer, has built-in redundancy and good heritage: Hershel IR at L2, Plank microwave background, and Aeolus wind sensors. Option 2 is shown in figure 11: the Space Micro Inc. Proton 400 computer suite, which offers a low mass solution using the cPCI bus architecture and good radiation hardening technology. However, it has lower TRL due to the required system level development. The Proton 400 computer solution was selected for lower mass and newer technology. The spacecraft bus includes additional data storage units for recording 128 Gbits. At 128 kbps, only 11 Gbits are required for 24 hr of data storage. 128 Gbits will provide 11 days of storage. The Surrey data recorders are suggested, providing 128 Gbits/unit at 150 Mbps.

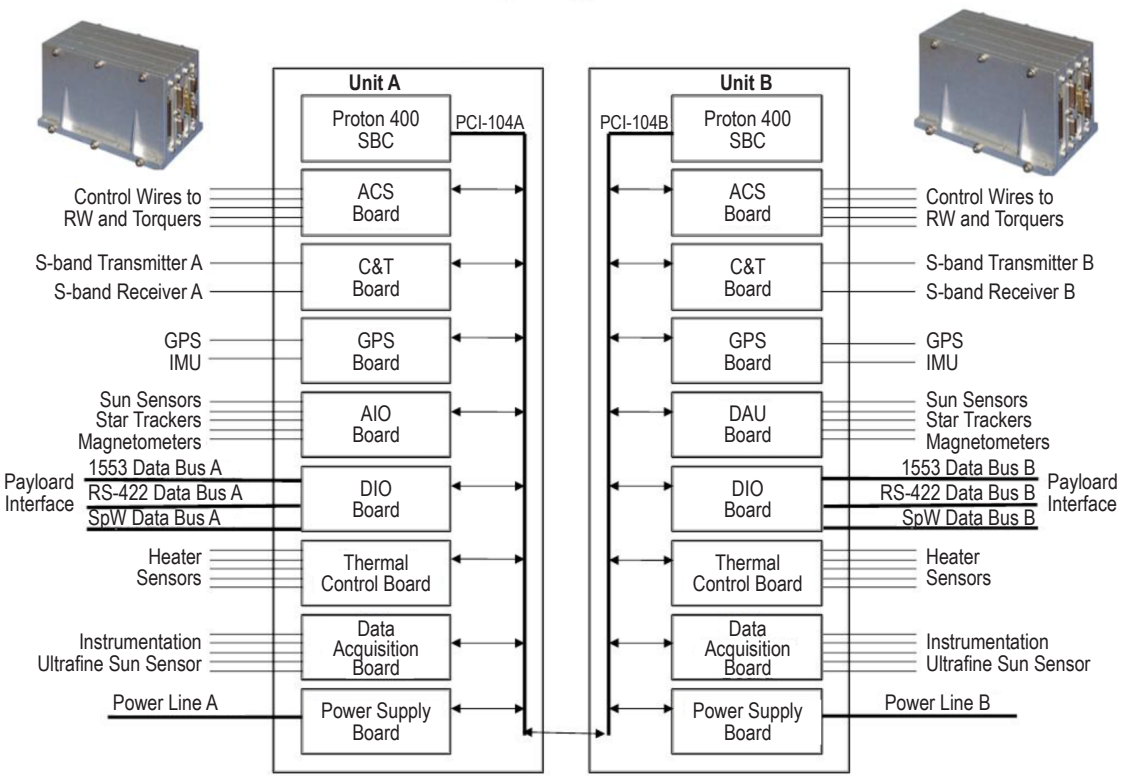

Figure 11. Spacecraft flight computers (low mass new technology solution).

7.4.2 Communications

Using the DSN, 11-hr average link times are provided by ground stations with overlapping coverage. Following Chandra's downlink strategy of three links per day (every 8 hr) at 1 Mbps, 3.7 Gbits (128 kbps×8 hr) can be downlinked in 60 min using S-band to a 34-m dish. Occasional DSN blind spots at perigee (approximately 2 hr) can be worked around in a 64-hr period. Spacecraft housekeeping/engineering data are assumed to be 5 kbps, which adds little to the data rate. A trade on S-band communication systems was also performed, the options shown in figure 12. Option 1 used L3 transmitter and receiver units, which have good heritage. Option 2 used the Aero-Astro transceiver package with a 5-W amplifier. It offers a low-mass solution using newer technology and some heritage; however, its availability is questionable. The L3 solution (option 1) was selected to reduce program risk.

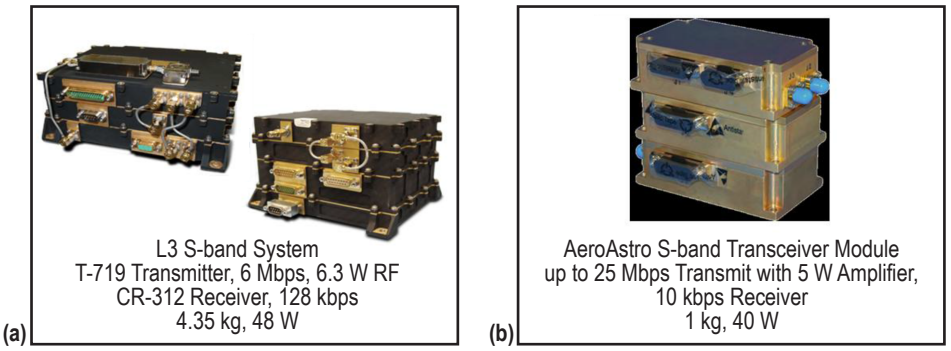

Figure 12. Spacecraft communication system trade: (a) Option 1 and (b) option 2. Option 1 was selected for risk reduction.

With 128 kbps of data collection for 8 hr, 3.7 Gbits are to be downlinked. Using Chandra's 1.024 Mbps link rate, 60 min of link time are required (3.7 Gbits/1.024 Mbps = 3,614 s (60 min)). Thirty minutes of link time would require twice the data rate (2.05 Mbps). 1.024 Mbps can be linked to a 34-m DSN dish with a 5-W transmitter, calculated at a worst case (apogee) distance of 133,000 km apogee. 4.5 db of margin is provided, where only 3 db is required. 2.05 Mbps would require twice the power: 10 W. Omniantennas are sufficient for the given data rates; no pointing dish or mechanism is required. Using S-band provides the least rain attenuation and space losses. A 10-W transmitter would be needed if an X-band is used giving the same availability.

7.4.3 Guidance, Navigation, and Control

Assuming an HEO similar to Chandra, no ultrafast pointing maneuvers will be required for Sun avoidance. The 60-deg Sun avoidance maneuvers can be done in 5 min, which exceeds the mission expectations. No Earth/Moon avoidance is required. Continuous science pointing duration of up to 100,000 s (28 hr) is desired, but interruptions for Sun avoidance as well as Earth and Moon occultation is acceptable. A minimum fast slew rate of 12 deg/min (120 deg in 10 min) once per orbit is desired. A slow scanning mode at 2.7 arcsec/s (2.7 deg/hr) up to 40,000 s (11 hr) is also

desired, meaning 11 hr of uninterrupted data collection. There are no rolls allowed for thermal or power management during science observations. The reaction control system (RCS) will be used for reaction wheel desaturation.

The reaction wheels selected from a previous study—the Advanced X-ray Timing Array (AXTAR)[4]—should be sufficient to achieve the WFXT operational slew rate of 12 deg/min and the continuous 11 hr of scanning. With a total mass of 2,500 kg, AXTAR had a slew capability of 12 deg/min with margin and achieved 28 hr of pointing. Some selected components of the WFXT conceptual design GN&C subsystem are shown in figure 13. Four RSI 68-170 Teldix reaction wheels by Rockwell Collins are used with 17 Nms momentum and 0.2 Nm torque for each wheel. Two Goodrich HD1003 star trackers are used to achieve 2 arcsec pointing knowledge. Two ultra-fine Sun sensors (UFSSs) are added to the guidance system to meet the 1-arcsec pointing knowledge required for slow scanning mode. They were used on the Hinode solar mission with a 0.15-in capability and a 31-Hz update rate. The Ball Aerospace High Accuracy Star Tracker (HAST) is another option. Used on Chandra, with a 0.15-in accuracy also but only with a 2-Hz update rate, HAST has possible cost issues. To achieve the 0.8-arcsec per 1/3-s jitter requirement, an active vibration isolation system was added to isolate the reaction wheels, which is the same system used on the Chandra telescope. Also, any movement of spacecraft components during science observations is restricted. No science is expected during desaturation of reaction wheels.

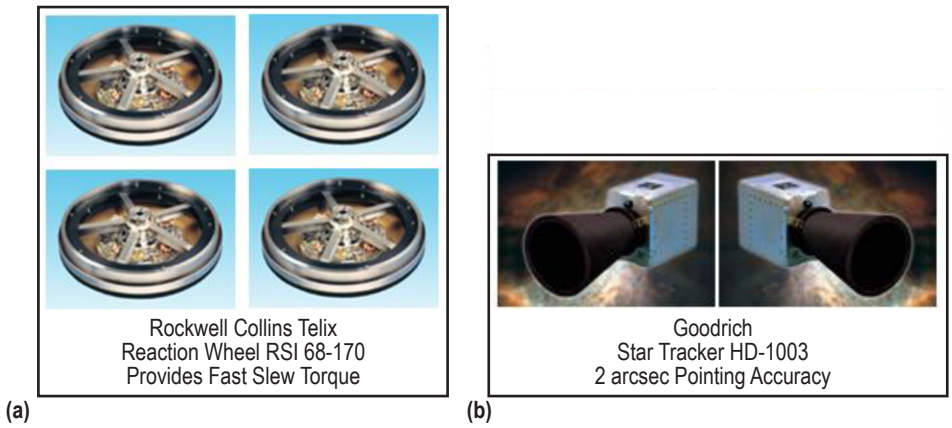

Figure 13. Major GN&C subsystem components: (a) Rockwell Collins Telix reaction wheel RSI 68-170 and (b) Goodrich star tracker HD-1003.

7.4.4 Avionics Trade Results

Some modifications would be required on the Saab Ericsson computer, bringing the TRL level down to 8, but the Space Micro computer will require significant system level development even though many of the individual boards have flight heritage, making its TRL level 6. Data acquisition boards were added to the Space Micro computer suite, allowing for the elimination of two dedicated units in the Saab Ericsson configuration. Elimination of these two data acquisition units (DAUs) saved a total of 8 kg in addition to the 6 kg saved using the Space Micro computers.

The possibility exists that the Space Micro data acquisition boards will be insufficient to handle all the instrumentation required in the end spacecraft design. At 150 g each, an additional two boards would only be an additional 300 g to the Space Micro design. The avionics subsystem components are listed in table 9.

Table 9. Avionics subsystem MEL.

WFXT				Quantity	Unit Mass (kg)	Basic Mass (kg)	Contingency (%)	Contingency (kg)	Predicted Mass (kg)
4.0	Avionics					161.86	30	48.56	210.42
	4.1	C&DH				73	30	21.9	94.9
		4.1.1	Flight computer	2	6	12	30	3.6	15.6
		4.1.2	Solid state recorder	2	1	2	30	0.6	2.6
		4.1.3	RCS controller	1	5	5	30	1.5	6.5
		4.1.4	RW controller	1	5	5	30	1.5	6.5
		4.1.5	Instrumentation	1	15	15	30	4.5	19.5
		4.1.6	Avionics and cabling	1	34	34	30	10.2	44.2
	4.2	GN&C				70.7	30	21.21	91.92
		4.1.1	Coarse Sun sensor	6	0.03	0.2	30	0.06	0.27
		4.1.2	Horizon sensor	2	1.1	2.2	30	0.66	2.86
		4.1.3	Star tracker	2	3.5	7	30	2.1	9.1
		4.1.4	UFSS	2	3.2	6.4	30	1.92	8.32
		4.1.5	Inertial measurement unit	2	0.8	1.5	30	0.45	1.95
		4.1.6	Reaction wheel	4	8.9	35.6	30	10.68	46.28
		4.1.7	Reaction wheel isolation system	4	4.5	17.8	30	5.34	23.14
	4.3	Communications				18.16	30	5.45	23.61
		4.1.1	S-band antenna	2	0.5	1	30	0.3	1.3
		4.1.2	S-band transmitter	2	2.3	4.6	30	1.38	5.98
		4.1.3	S-band receiver	2	2.1	4.1	30	1.23	5.33
		4.1.4	S-band switch	1	0.2	0.18	30	0.05	0.23
		4.1.5	S-band filter	2	0.1	0.18	30	0.05	0.23
		4.1.6	S-band diplexer	2	0.5	1	30	0.3	1.3
		4.1.7	GPS unit	2	1	1.9	30	0.57	2.47
		4.1.8	GPS antennas	4	0.1	0.2	30	0.06	0.26
		4.1.9	Coaxial cabling, miscellaneous	1	5	5	30	1.5	6.5

7.5 Power

The conceptual spacecraft design was actually completed in two sessions, with the first session being a very quick design that was not optimized and was to give an idea of feasibility. The design team started the second session of this study with a baseline power system design from the first session that closed to all requirements. The object of the second study session was to investigate improvements to the system to arrive at a definitive prephase A design.

The first order of business was to sort out requirements. The design team started by carrying forward the requirements from the first study session and modified those in light of the improved (shorter) eclipse times from the mission analysis trades. The GR&A that guided the design is listed in table 10.

Table 10. Power subsystem GR&A.

Category	Value
Power subsystem required to provide power for all spacecraft elements + payload power.	Vehicle will provide capability to store, generate, manage/condition, and distribute power to all subsystems and payloads on the vehicle.
Operation orbit	16,000 × 133,000 km
Bus voltage	28 V nominal
Power during initial checkout/solar array deployment	Power will be provided to all attached architecture elements during initial checkout (1 hr) and solar array deployment if required.
Payload circuits	20 switched circuits provided to payload
Overload protection	Will be provided for all critical functions (should consider resettable fuses).
Fault tolerance	No single fault will allow the vehicle to enter mission critical failure mode.
Ground reference	A common ground reference will be provided across all subsystems.
Secondary battery charge/discharge efficiency	95%
Secondary battery maximum depth of discharge	60%

The design team traded two new power electronics options and numerous lithium-ion batteries in an attempt to reduce mass and improve reliability.

The original Southwest Research Institute (SWRI) fully integrated power system was chosen mainly because it is a high-heritage, easily configured, middle-of-the-road solution. Early models had some latch-up problems that SWRI claims to have solved. This is a safe choice when the designers do not have time to trade other solutions.

BroadReach goes to an even higher level of integration by combining power electronics and avionics into a single extremely low-mass package. It is very cheap as well. The experienced integrators that the design team consulted with, however, did not recommend it for use outside of LEO because of its low levels of radiation shielding.

Because the MESSENGER mission trajectory had an extremely high characteristic energy and required some 6 yr to reach the mission destination (Mercury), the power system electronics had to be both very light and very robust. The Applied Physics Laboratory design met these demanding requirements by integrating the array regulation, battery charge, and power conditioning functions into one enclosure while packaging the power distribution in another. This 'partial integration' approach allowed full redundancy for all mission critical functions while minimizing structural mass (enclosure, bus bar, etc). Of course, it is not the least expensive solution.

The team chose the MESSENGER solution because it was very robust and yet reasonably low mass. The one major area in which the MESSENGER power system required modification

was energy storage. MESSENGER carried H2 secondary batteries for environmental reasons. The design team chose lithium-ion secondary batteries instead; note that the battery charger boards in the integrated power electronics box will have to be modified to charge these batteries. The design team traded a number of specific batteries for this application and chose the ABSL 24AH-ABS-DW-1001 aerospace battery chiefly because of its energy density, heritage, robust packaging, and general reputation among integrators.

The power subsystem components and masses are listed in table 11.

Table 11. Power subsystem MEL.

Component	Quantity	Unit Mass (kg)	Total Mass (kg)	Contingency (%)	Predicted Mass (kg)
Solar array wing	2	6.6	13.2	30	17.2
Solar array wing structure and mechanisms	2	3.6	7.2	30	9.4
Solar array drive actuator	2	0.7	1.4	30	1.8
Integrated power electronics box	1	6.6	6.6	30	8.6
Power distribution unit	1	11.5	11.5	30	15
Secondary batteries	12	6.5	78	30	101.4
Cabling	1	11.7	11.7	30	15.21
Total			129.6	30	168.5

Compared to the results from the first design session, the reduced eclipse period provided by the updated orbit orientation reduced the energy storage requirement but increased the battery charge power requirement. Trades reduced power electronics mass by 27% with no loss in reliability. The secondary battery trade increased effective energy storage density by meeting the requirement more closely and by reducing the mass of the required redundant battery. The overall result is a lighter, yet more robust power system.

7.6 Structures

The concept study was actually completed in two sessions, with the first session focusing on a quick analysis to check the feasibility of the mission concept. The analyses performed in the second session of the WFXT study built on those performed previously, employing the same tools and approaches where possible. The second session analysis added fidelity by incorporating additional features and considering additional structural criteria like stiffness and stability.

It should be noted that the study did not address thermal expansion. This is probably not a driving issue, but something that would need to be looked at in a full-up design activity as it could affect internal stresses and, potentially, telescope alignment.

The GR&A used in the structural assessment is listed in table 12. Since it is assumed that there will not be a dedicated test article to verify the structural adequacy, the yield factor of safety for metallic materials was set to 1.25 (protoflight) in accordance with NASA-STD-5001A.[5] Additionally, a requirement for natural frequency is specified to ensure that there is no dynamic coupling between the structural modes of the telescope and the launch vehicle. At the time this study was initiated, a specific launch vehicle had not yet been selected, so a conservative value of 35 Hz was assumed.

Table 12. Structures subsystem GR&A.

Category	Value
General	Primary structure will be designed to meet the launch load requirements. Secondary structure is assumed to be 20% of the weight of the primary structure. Joints and fittings are assumed to be 50% of the primary structural weight.
Load cases	Primary loads to be assessed are –5 g axial and ±2 g lateral in 45 deg increments.
Factor of safety for composite materials	Yield factor of safety: N/A Ultimate factor of safety (uniform areas): 1.5 Ultimate factor of safety (discontinuity areas): 2
Factor of safety for metallic materials	Yield factor of safety: 1.25 Ultimate factor of safety: 1.4
Factor of safety for propellant tanks	Yield factor of safety: 1.25 Ultimate factor of safety: 1.4 Proof pressure factor of safety: 1.05XMEOP Burst pressure factor of safety: 2.0XMEOP
Natural frequency	Natural frequency of structure to be at least 35 Hz in axial and lateral directions.

Finite element mapping and postprossessing (FEMAP) was used in combination with NASTRAN to develop a finite element model (FEM) of the WFXT structure. As the design evolved to a smaller bus from session 1 to session 2, a new FEM was required. Care was taken in the development of the new FEM to use the same modeling methods and assumptions where possible.

As previously stated, the session 2 study added fidelity to the structural assessment by incorporating additional features into the model. Figure 14 shows a side-by-side comparison of the session 1 and session 2 FEMs, identifying the additional structure represented in session 2. It should be noted that the new telescope cones, CCD masses, and the launch restraint fittings were not optimized or analyzed in this study. They were included in the model to approximate the flexibility of the integrated structure so that the stiffness of the assembly in the launch configuration could be assessed and the rear support structure could be sized.

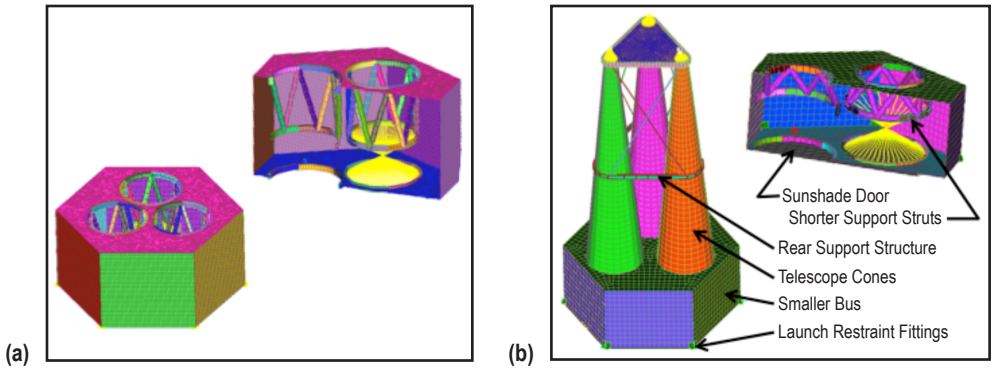

Figure 14. Comparison of the two FEMs from (a) session 1 and (b) session 2.

The session 2 study repeated the structural assessment performed in session 1 using HyperSizer optimization software. The program performs closed-form margin of safety calculations using results from the FEMAP FEM. The code then iterates specified design parameters with NASTRAN to resolve any negative margins and reduce overly conservative margins. The resulting optimized configuration was then read back into FEMAP, and another complete finite element analysis was performed.

Beyond the failure modes and design parameters considered in session 1, the session 2 study also included an assessment of the structural stability (buckling) and expanded the trade space to consider additional materials and panel constructions.

The optimized materials and design parameters for the session 2 structure are nearly identical to the results of the session 1 study. This shows that the session 1 and session 2 models behave similarly and adds a degree of confidence in the results.

The final structural masses are shown in the MEL in table 13. In spite of the increased factor of safety and the new natural frequency requirement, the session 2 mass is still significantly lower than what was determined from session 1. This is largely due to the smaller bus size and shorter telescope support struts (less metal, less weight).

Table 13. Structures subsystem MEL.

Category	Quantity	Unit Mass (kg)	Basic Mass (kg)	Contingency		Predicted Mass (kg)
				(%)	(kg)	
Structures total			384.36	30	115.31	499.67
Primary structures	1	159.7	159.7	30	47.91	207.61
Secondary structures	1	31.9	31.94	30	9.58	41.52
Telescope support rings	1	7	7	30	2.1	9.1
Telescope support struts	1	5.2	5.2	30	1.56	6.76
Rear support structure	1	18.7	18.7	30	5.61	24.31
Sunshade door	1	70.1	70.1	30	21.03	91.13
Joints and fittings	1	50.5	50.5	30	15.15	65.65
Miscellaneous hardware and brackets	1	41.2	41.22	30	12.37	53.59

The analysis shows that the structure of the WFXT can be fabricated with materials and methods common in the aerospace industry. This will allow the structure to be developed with minimal costs and maximum reliability.

It is suggested that if work of WFXT be continued, an effort should be made to represent the nonstructural masses (propellant tanks, avionics, etc.) to better represent the geometry and materials of the telescope cones, and include thermal properties of the materials and loads used in the FEM. While this will not likely change the structural mass significantly, it would allow a more thorough assessment of the structural performance and an understanding of any telescope alignment issues resulting from thermal growth/contraction.

Another suggestion is to consider the use of composites, particularly for the sunshade door. While the door is not truly a structural component, it was driven to a relatively heavy design to satisfy stiffness requirements. A composite sandwich configuration will likely provide a much better stiffness-to-weight solution than the flat, orthogrid or isogrid metallic panels considered in this study. The reduction in weight offered by composites would then need to be traded against the costs associated with development of the panels. The long-term impact of cold, radiation, and meteoroid impact would also have to be considered.

7.7 Thermal System

A passive thermal design concept was developed for the WFXT spacecraft bus. Thermal control will utilize high-TRL components, including multilayer insulation (MLI), high-emissivity paint and coatings, heatpipes, heaters, etc. to maintain spacecraft subsystem components within acceptable temperature ranges. There are no dedicated radiators; however, spacecraft structural panels act to dissipate avionics heat by conduction and also act as radiative surfaces. The orbiter bus outer surfaces are covered in low-absorptivity materials in order to cold bias the structure. Cold biasing the structure will serve to minimize thermal gradients due to environmental loads and therefore, minimize expansion and contraction of the structure.

A propellant tank located within the orbiter is wrapped in MLI, and a thermostatically controlled tank heater is utilized as needed. RCS thrusters, antennas, and solar array mechanisms are not part of the prephase A analysis. Temperature prediction of experiment boxes, including the digital processing assembly (DPA), are not part of the analysis.

Thermal control GR&A is shown in table 14 for the WFXT study. The telescopes are assumed thermally isolated from the spacecraft for the purpose of preliminary analysis. The DPA is located on the spacecraft and is assumed to dissipate 20 W to the spacecraft structure. Thermal control mass estimates for the heatpipe/cold radiator assembly used to maintain each CCD focal plane assembly at –90 °C were taken from Chandra data and represent redundant systems.

Table 14. Thermal subsystem GR&A.

Category	Value
Spacecraft thermal control	Passive thermal control of the spacecraft shall utilize MLI, heaters, thermostats, radiators, heatpipes, etc. to maintain spacecraft subsystem components within acceptable ranges.
Experiment temperature prediction	Experiment temperature prediction is not included as part of the subsystem analysis.
Experiment heat rejection	Experiment is assumed thermally isolated from the spacecraft with the exception of one DPA located on the spacecraft. DPA will dissipate 20 W. Thermal control mass estimates will include sizing a heatpipe/cold radiator assembly to maintain each CCD focal plane assembly at –90 °C. Heat dissipation to each cold radiator is 4 W per telescope.
Environment heat loads	Environment heat loads will be calculated for Chandra-type HEO (16,000 × 133,000 km altitude). Sun avoidance angle is 45 deg. Minimum and maximum beta angles to be analyzed.

Environment heat loads were calculated for beta angles of 0 and 50 deg. This range envelopes the predicted minimum and maximum expected during the duration of the mission for mission analysis parameters. A Sun avoidance angle of 45 deg drove the spacecraft orientation.

The proposed spacecraft bus layout is shown in figure 15, including avionics and power systems boxes, the propellant tank, and reaction wheels. The thermal model heat loads are located based on this configuration. The sunscreen is not shown for clarity, but serves to shield the telescopes completely from direct sunlight.

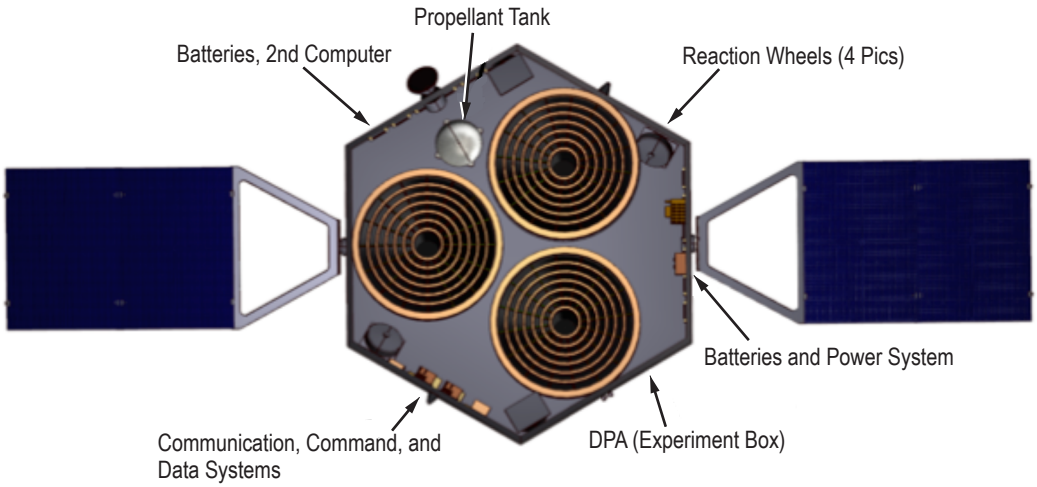

Figure 15. Illustration showing the subsystem component locations.

A system-level thermal model of the spacecraft orbiter bus structure was developed using Thermal Desktop® to assess support structure, solar array, and subsystem equipment interface temperatures. The structure is modeled as aluminum, and the panel thickness is consistent with the structural design. Environment heat loads were calculated for a Chandra-type orbit (16,000×133,000 km altitude). Subsystem component heat loads were imposed directly on the bus

structure. Box level details were not considered in these analyses. Orbital-averaged, steady-state spacecraft structure temperatures were generated in order to determine a range of component-to-bus interface temperatures to be expected during the course of the flight. Temperatures are shown in figures 16 and 17 for the 0 and 50 deg beta angle cases, respectively.

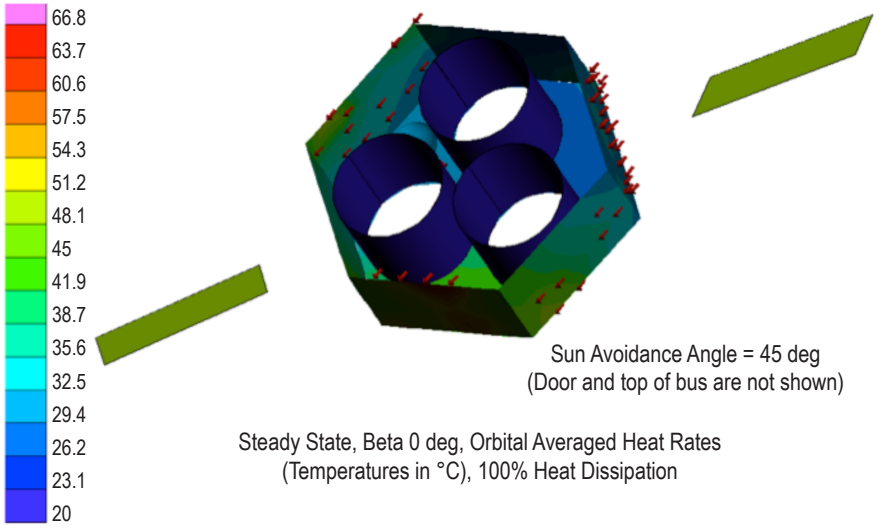

Figure 16. Steady state spacecraft bus predicted temperatures for a beta angle of 0 deg.

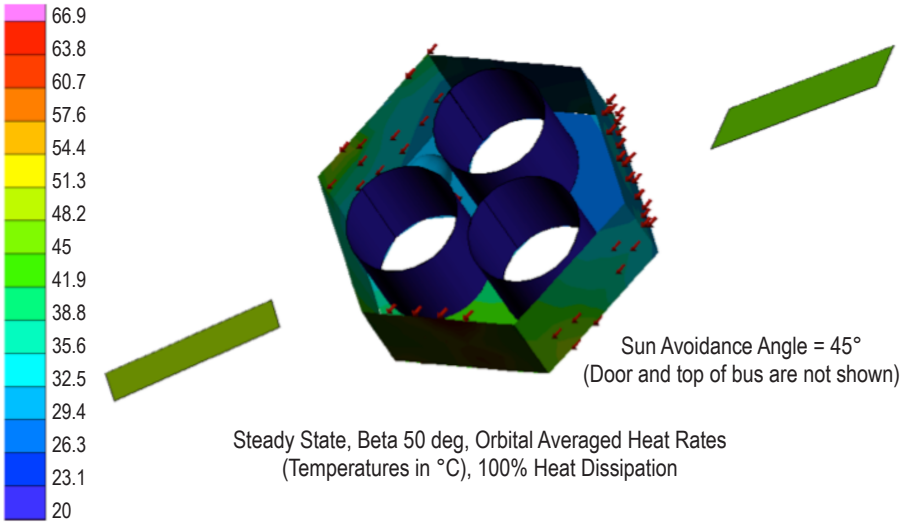

Figure 17. Steady state spacecraft bus predicted temperatures for a beta angle of 50 deg.

A summary of the predicted and operating interface temperature range for the avionics and power systems equipment and reaction wheels is shown in table 15 for the operational mission phase for beta angles of 0 and 50 deg. All predicted interface temperatures are within acceptable range.

Table 15. Summary of predicted temperatures and acceptable operating temperatures for beta angles of 0 and 50 deg.

Category	Predicted Temperature Range Beta Angle = 0 deg	Predicted Temperature Range Beta Angle = 50 deg	Operating Temperature Range
ACS control system	35.6 °C to 45 °C	35.6 °C to 51.3 °C	–40 °C to 85 °C
Reaction wheels (4)	20 °C to 41.9 °C	23.1 °C to 41.9 °C	–20 °C to 60 °C
Command and data system	35.6 °C to 66.8 °C	35.6 °C to 66.9 °C	–40 °C to 85 °C
Communications system	35.6 °C to 54.3 °C	35.6 °C to 66.9 °C	–20 °C to 70 °C
Power systems	20 °C to 29.4 °C	20 °C to 26.3 °C	–40 °C to 85 °C
Batteries	17.3 °C to 29.4 °C	20 °C to 26.3 °C	0 °C to 45 °C
RCS tank	20 °C	20 °C	10 °C to 30 °C
DPA (experiment equipment)	20 °C to 29.4 °C	20 °C to 29.4 °C	–40 °C to 85 °C
Solar arrays	48.1 °C	48.2 °C	–50 °C to 75 °C

Optical properties used in the thermal model are itemized in table 16. The spacecraft bus internal surfaces are assumed to be black annodized to optimize radiative exchange within the enclosure. Silverized teflon is used as an outer layer on the MLI blankets covering external surfaces of the bus. MLI effective emissivity (ε^*) values represent effective emissivity for the insulation blanket.

Table 16. Optical properties used in the thermal model.

Category	Material	Absorptivity	Emissivity
Spacecraft bus internal surfaces	Black annodized	0.9 (2)	0.9 (2)
Spacecraft bus external surfaces, sunshade door	Silverized teflon ε^*= 0.03 (4)	0.07 (3)	0.82 (3)
Telescope mirror to bus interface	2 mil Al MLI ε^*= 0.002 (4)	0.12 (3)	0.03 (3)
RCS tank	ε^*= 0.03 (4)	0.12 (3)	0.03 (3)

White paint, uncoated beta cloth, and silverized teflon were considered for exterior materials on the spacecraft bus. Silverized teflon proved a better material due to its ability to cold bias the bus and minimize thermal gradients.

Table 17 details the subsystem equipment dimensions and estimated power level. A total of 416.6 W of spacecraft power/heat dissipation was considered, and this includes 1 W of heater power for the propellant tanks. All heat loads are imposed directly on the structure and modeled as area-averaged heat loads. The DPA is an experiment box that dissipates 20 W to the structure.

Table 17. Subsystem and experiment box dimensions and heat dissipation.

Category	Dimensions Per Unit (Maximum)	Total Power (W)	Quantity
ACS control system IMU assembly	$0.09 \times 0.09 \times 0.09$	24	1
Reaction wheels and isolation system	0.347 dia. $\times$ 0.248	105.6	4
Command and data system flight computer	0.162×0.155 x 0.102	108	2
Command and data system data recorder	$0.32 \times 0.17 \times 0.055$	30	2
Command and data system RCS controller	$0.2 \times 0.15 \times 0.1$	10	1
Command and data system RW controller	$0.2 \times 0.15 \times 0.1$	10	1
Communications system S-band transmitter	$0.19 \times 0.14 \times 0.101$	48	2
Communications system S-band receiver	$0.165 \times 0.14 \times 0.107$	16	2
Power systems enclosure	$0.286 \times 0.196 \times 0.142$	10	1
Power dissipation unit	$0.234 \times 0.226 \times 0.239$	13	1
Batteries	$0.349 \times 0.192 \times 0.092$	20	12
RCS tank	Sphere (Rad=0.25)	1 W heater	1
DPA (experiment equipment)	$0.23 \times 0.18 \times 0.18$	20	1
Total		416.6	

Thermal control mass estimates for the WFXT spacecraft are shown in table 18. Total thermal control mass for the configuration is estimated at 35.1 kg, which includes a 30% margin.

Table 18. Thermal subsystem MEL.

Category	Quantity	Unit Mass (kg)	Basic Mass (kg)	Contingency		Predicted Mass (kg)
				(%)	(kg)	
Thermal total			27	30	8.1	35.1
MLI/thermal tape	1	15	15	30	4.5	19.5
Thermal filler/spreader/ heatpipes	1	4.5	4.5	30	1.35	5.85
Paint/thermal coatings	1	3	3	30	0.9	3.9
Heaters/thermostats	1	1.5	1.5	30	0.45	1.95
Cold radiator and heatpipe assembly	3	1	3	30	0.9	3.9

Based on a preliminary, prephase A level analysis, all interface temperatures are within acceptable range for the defined orientation and mission phase. Thermal management is accomplished with typical flight-proven components, and no technology development is required.

Recommendations for future work include generating a more detailed analysis of the avionics and power systems. Box-level geometry, timelined power estimates, and heat capacitance should be added to the model in order to perform transient analyses. A parametric study of beginning-of-life and end-of-life optical properties should be conducted to determine the impact of thermal surface degradation over mission life. Hot and cold bounding cases should be analyzed to determine the full scope of likely temperature excursions during nominal and off-nominal events. Reduced subsystems power cases would be helpful to assess off-nominal operations.

8. RISK ANALYSIS

Taxonomy-based risk identification works well for prephase A studies because it can be tailored to drive out the specific uncertainties that can undermine the decisions that the design team makes in prephase A. For spacecraft design, these include uncertainties in derived requirements (what assumptions are made in absence of hard data?), in the choice of components that have little space heritage, in the availability of components, in test planning for components and integrated systems, and in the integration of the spacecraft as a whole.

The ACERT tool simply asks questions to assess these uncertainties and to suggest possible risks. Its real value is that it assures that the design team considers a number of specific, relevant risk sources for every component and flight operation. The risks identified are presented in table 19.

Table 19. Identified risks for WFXT.

Statement	Context	Mitigation Options
If high speed data recorder is exposed to high radiation levels in the Van Allen belts or in the areas beyond them, it may fail, resulting in a loss of data.	The data recorder has been rated to only 5 kRad radiation dose, suggesting that it was designed for use in LEO. It should be tested and qualified for the environment in which it will be operated.	Recorder may be redesigned to use radiation–hardened components, or shielded. Unit should then be requalified. Optionally, use another recorder that is qualified for environment.
If Surrey SGR-20 GPS receiver is exposed to high radiation levels in the Van Allen Belts or in the areas beyond them, it may fail.	The GPS receiver has been qualified for radiation dose of 10 kRad, suggesting that it was designed for use in LEO. It should be tested and qualified for the environment in which it will be operated.	Receiver could be shielded and unpowered outside LEO. Unit could be then requalified for this environment. Different unit could be substituted.
If the 3-junction gallium arsenide photo-voltaic cells in the solar arrays experience high-energy radiation while travelling through the Van Allen belts, they may degrade more rapidly than anticipated, resulting in a reduction in power.	High efficiency triple junction cells have not been qualified for an environment in which they are exposed to high levels of ionizing radiation repeatedly and regularly over the life of a long mission. Thus, there is insufficient data to predict the rate at which the performance of these cells will decrease over time in such an environment.	Additional qualification testing should be done during phase A study to determine degradation rates. If degradation is severe, there is the option of simply using more robust single junction cells.
If the radiation environment degrades thermal coatings on the spacecraft and insulation, temperatures may rise beyond required maximum operational temperature, resulting in partial loss of mission.	Degradation of MLI and optical coatings designed for thermal control was a significant problem for the Chandra mission, which was flown in a similar orbit. This degradation was attributed to radiation exposure in the Van Allen radiation belts.	Research is needed to find coatings and insulation that are more resistant to ionizing radiation. These must then be qualified for the unique mission environment.
If the x-ray mirrors are not damped and supported properly, they may be damaged by vibration during launch.	The x-ray mirrors proposed are much thinner and more closely spaced than previously flown mirrors. No complete dynamic analysis has been performed on the mirror assembly, so mirror configuration has not been qualified.	Complete dynamic analysis should be performed as part of the phase A study and a suitable configuration settled. This should resolve the risk.
If the instrumentation team is unable to develop the required x-ray mirrors within the cost and schedule constraints of the mission, science objectives may be severely compromised.	The x-ray mirrors must be designed and polished using a process that has not been fully developed. Open technology challenges remain.	Significant issues research should be performed to plan the development effort and to resolve uncertainties. Technology gap analysis completed in this study is the first step in this process.

Because the x-ray mirrors required a significant development effort, the design team recommended that a technology gap analysis was performed to determine the degree of development difficulty in completing and qualifying this component.

Table 20 shows the number of risks found in each of the 25 risk categories of a typical risk matrix. Most of the risks found are fairly low in both risk probability and possible impact. One, however, is right in the very center of the space. This is the development risk for the x-ray mirrors. This is the focus of the technology gap analysis, performed separately.

Table 20. Summary of risk analysis.

	1 Very Low Impact	2 Low Impact	3 Moderate Impact	4 High Impact	5 Very High Impact
5 Very Likely					
4 Likely					
3 Somewhat Likely	2		1		
2 Not Likely	2				
1 Very Unlikely			1		

In summary, the vast majority of the risks involve Van Allen radiation belt transit and telescope development risks. Although there are few risks, they are significant at this point in the design cycle. A technology gap analysis will provide much further insight into the telescope development risks. Van Allen belt environment should be a significant focus during the phase A study.

9. TECHNOLOGY GAP ANALYSIS

The intent of this analysis was to provide an assessment of the current state of readiness for the technologies and processes required to build the 'telescope detector module' or 'optics module' for the WFXT spacecraft. All other technologies required for the spacecraft were deemed to be high TRL and therefore were not assessed as part of this analysis. To perform this analysis, the design team took inputs from several sources, including the original science instrument design team as well as many online resources for researching analogous technologies and applications. The readiness level of each item in the assembly was assessed against known technologies. A subelement level MEL was provided by the WFXT science instrument design team to support this assessment. After assessing the readiness level of all items, those with readiness levels below 6 were subject to a more in-depth assessment of the plan to raise the readiness level to 6 for use in this application. This technology development assessment was performed using a combination of TRL, Manufacturing Readiness Level (MRL), and Research and Development Degree of Difficulty ($R\&D^3$) metrics.

TRL is a standard NASA metric used to assess the readiness of a particular technology.[6] Technologies are assessed on a scale from 1 to 9 where 1 is a demonstration of basic principles and 9 signifies a flight-proven technology. In general, the TRL is a good metric for assessing how ready a particular technology is for use in a particular design. A TRL of 6 is traditionally identified as the transition point from technology development to application-specific subsystem or system development. This system development is considered part of a typical spacecraft development program. Therefore, program managers will seek technologies with TRLs above 6 for use in their missions, and selecting technologies below 6 requires an additional technology development budget before traditional mission planning and development budgets can be employed.

Similar to TRL, the MRL assesses the readiness of manufacturing processes.[7] This metric is more commonly employed by the Department of Defense to assess manufacturability of new weapons systems, but the principles apply to any manufacturing problem. The MRL values loosely correlate to the TRL values as they relate to the system lifecycle, with a 1 representing a very basic process and a 9 representing a well-established mass production process. The additional MRL 10 identifies mature processes that have been streamlined through the implementation of Lean principles. Processes typically transition from development to implementation and improvement between MRL 6 and 7, similar to the transition from technology development to engineering development at TRL 6. MRL was added to the assessment of the WFXT science module due to the high dependence on repeatable manufacturing processes for the development of the mirror assembly.

The $R\&D^3$ is a metric used to quantify the probability of successfully completing a research and development or technology development effort.[8] This metric uses Roman numerals ranging from I (which represents a low difficulty, high probability of success technology program) to V (which represents a very difficult, low probability of success technology development program).

An assessment of the R&D^3 is based partially on the presented technology development plan and partly on the assessment of how significant a departure the proposed technology is from current technologies. In theory, as a technology development program matures, the R&D^3 metric will be reevaluated and should progress toward a rating of I.

Table 21 provides an overview of the TRL/MRL and R&D^3 evaluation for the subsystems and components of the instrument portion of the WFXT spacecraft. This general overview shows that much of the telescope detector module is based on high TRL technologies that have been widely demonstrated on previous missions. NASA has flown many space telescopes over its 50+year history, and many of the general requirements for optical systems of this size are common between these various missions, providing a rich heritage of technologies to draw upon. The exceptions in this case are related to the manufacturing and assembly of the unique mirror structure required for the WFXT mission.

Table 21. Technology gap summary.

Component	TRL/MRL	R&D^3
X-ray telescope	3–4	II
FMA primary structure assembly	4	II
Top spider	8	–
Bottom spider	8	–
Outer case	8	–
Mirror mounting hardware	4	II
Miscellaneous hardware	8	–
Fused silica mirror shells	3–4	I–II
Thermal precollimator	8	–
Optical bench	8	–
Structure	8	–
Thermal control	8	–
Fine attitude sensor	8	–
Star tracker	8	–
X-ray detector assembly	7–8	–
Detectors (2×2 CCD)	7–8	–
Detector thermal control	7–8	–
Radiator	7–8	–
Trim heater	7–8	–
Optical blocking filter	7–8	–

With the exception of the mirror mounting hardware and the fused silica mirror shells (discussed below), the x-ray telescope assembly is based on high TRL technologies. The top and bottom spider assemblies provide structural support at each end of the mirror shell assembly. This approach to x-ray mirror mounting has been employed on several missions, most recently on the XMM/Newton observatory launched in late 1999. While a new design is required to meet the size

and shape requirements of the WFXT mission, the technology is well understood and will require no technology development. The outer case is similar in design but smaller than the case flown on the Chandra X-ray Observatory launched in 1999. The thermal precollimator uses the same technology used in the XMM/Newton optical system and is flight proven.

The optical bench assembly is also rated at a high TRL. The structure, like the telescope outer case, is very similar in design and application to that used on the Chandra X-ray Observatory. The thermal control system for the optical bench uses the same technologies that were flown on the XMM/Newton spacecraft and the Swift spacecraft, launched in 2004. Additionally, extensive lab testing has been completed on these technologies in support of the JET-X program. These technologies are very well known and will require no further development for this mission.

The specifications made for the star trackers required for fine attitude determination are well within the capability range of commercially available star trackers. In addition, the knowledge requirements are an order of magnitude less demanding than those placed on the Chandra X-ray Observatory. There is no technology development required for this system.

The x-ray detector assembly designed for WFXT relies heavily on technologies previously flown on other x-ray telescope missions. The 2×2 CCD detector arrays are direct descendants of the MIT Lincoln Laboratory CCID17 (flown on Chandra) and CCID41 (flown on Suzaku).[9] The passive thermal control approach proposed for the detectors is widely employed by CCD arrays in a wide range of applications including space telescopes and other observation platforms. The blocking filter is similar to those used on Chandra.

The mounting of the mirrors in the flight mirror assembly (FMA) primary structure assembly presents unique challenges. This mission will be the first to use full-shell, thin glass mirrors. These mirrors are to be held in place by the end spider assemblies. While many current missions (XMM/Newton, Chandra, etc.)[10] have proven aspects of the mirror mounting technology,[11] the application of those technologies for this mission is unique and unproven. These full-shell optics must be held in place at the ends without presenting significant shape distortion. With the concept certainly having been proven and some work being completed on mounting approaches, a TRL value of 4 has been assigned to this technology.

The likelihood of successful development of the mirror mounting technology is very high. Several potential solutions exist. The application of these solutions will be unique to this mission; however, other concept studies have identified clear paths forward for development and testing.[12] This technology requirement represents a significant, but not extreme, extrapolation from existing capabilities and has been given an R&D[3] rating of II (probability of success = 90%).

The manufacturing of full-shell, thin glass mirrors for the WFXT mission presents a significant challenge. In this case, the design team has assessed the MRL for the processes required to produce the mirrors rather than the TRL. The technology of fused silica mirrors is well known, as are the technologies for polishing mirrors to very precise finishes. However, to produce precise finishes required for x-ray astronomy on very thin glass mirrors, new processes must be developed. The process has been proven in theory by a manufacturer in Milan, Italy;[1] however, the mirrors

used in the WFXT mission will be produced by a team at MSFC. This proof-of-concept process must be repeated and improved in the production facility in Huntsville, Alabama.

In order to advance the processes from a proof-of-concept (MRL 3) to system and subsystem production in a relevant environment (MRL 6), the processes must first be replicated by the production team at MSFC. This step will advance the MRL to 4. A demonstration of the repeatability of the process will advance the MRL to 5. A proof of the ability to produce the mirror shells at the rates required to support the WFXT mission plan will advance the MRL to 6 (faster production represents the relevant environment). From there, a typical program engineering development approach will refine the processes and advance the MRL to a sufficient level to support full-speed production in support of the mission. This plan has been articulated by the WFXT team and, while challenging, is anticipated to have a high probability of success.

The more difficult phase of the MRL advancement is getting from 3 to 5, where the MSFC team must replicate what has been proven in other facilities and then refine those processes to a repeatable maturity. This represents a significant but not extreme extrapolation of existing technologies and capabilities. This process will be completed using the commercially available Zeeko IRP600 multiaxis milling machine. The processes for polishing glass with this machine are very well known. The challenge for the development team is in customizing those processes to account for the thin nature of the WFXT glass shells. The R&D^3 rating for this step is II (probability of success = 90%). Once this is accomplished, the step to MRL 6 is a modest extrapolation of the processes already developed. In this step, those processes will be streamlined to speed up production. The R&D^3 rating for this step is I (probability of success = 99%).

10. LOW EARTH ORBIT ASSESSMENT

The design team was also tasked to complete a top-level assessment of the feasibility of the proposed spacecraft bus being used in LEO, an orbit that could possibly save money by allowing the use of a smaller launch vehicle. The proposed LEO is 600 km altitude with an inclination of 6 deg. Each subsystem discipline lead, except as noted below, was asked to use engineering judgment and estimate the changes, if any, that may be required for his or her subsystem to operate in the LEO environment. However, given the assumption that the additional propellant load for deorbit would probably dominate the required bus modifications, the mission analysis and the propulsion leads were asked to calculate the propellant loads for the LEO mission and size the propulsion system appropriately so that the configuration lead could ensure adequate bus volume. In addition to estimating the propellant required for controlled deorbit (assumed a requirement based on the mass of the observatory), mission analysis also included launch vehicle selection, orbital lifetime estimates, eclipse duration estimates, and beta angle histories so that other subsystem leads could consider these impacts on their designs.

10.1 Launch Vehicle Selection

The NASA LSP Web site provided performance estimates to LEO for inclinations down to 10 deg. The team used these values to extrapolate the performance to 6 deg for the Falcon 9 (version 1.1) vehicle launched out of Cape Canaveral Air Force Station. The resulting data are shown in table 22. The time allotted for the study was insufficient to get a performance quote from the LSP, but the extrapolated data should give a good estimate of performance to the target inclination. In addition, even though the LSP numbers are already conservative, the 15% performance reserve makes the estimate even more so. The estimated 3,390 kg payload capability of the Falcon 9 should be sufficient for a LEO mission.

Table 22. Falcon 9 performance to 600 km circular orbit for various inclinations.

Inclination (deg)	Payload (kg)
28.5	15,280
20	10,140
10	5,455
6	3,990 (est.)
Payload with 15% reserve = 3,390 kg	

10.2 Orbital Lifetime, Eclipse, and Beta Angle History

Orbital lifetime was given a quick analysis using STK and NASA's Debris Assessment Software. Based on the estimated spacecraft parameters, the 600 km altitude appears sufficient to avoid orbit decay and reentry prior to mission completion. One unknown, however, is the predicted solar cycle in 2020 and beyond, which could greatly influence the orbit lifetime and require either additional propellant for orbit maintenance or launch into a higher orbit. Eclipse and beta angle histories were also generated using STK, with the results being given to thermal and power analysts for consideration in their subsystem designs.

10.3 Controlled Reentry From Low Earth Orbit

Probably the most significant modification to the bus would come from the propellant necessary for a controlled reentry, a maneuver not required for the Chandra-type orbit. The approach for reentry is to slowly lower perigee down to 150 km with the first four propulsive maneuvers with a fifth maneuver targeting a flight path angle of –1.2 deg at 60 km altitude. The resulting ideal delta velocity (ΔV) values are 31.7 m/s for maneuvers 1 through 4 and 37.6 m/s for the final maneuver. Selecting the appropriate main propulsion system (MPS) and RCS thrusters and adding some gravity loss results in an overall propellant load of 314 kg, with 26 kg being reserved for momentum unloading.

10.4 Resulting Propulsion System

A monopropellant hydrazine blowdown propulsion system is designed to accommodate 314 kg of maneuver propellant. This system is responsible for the momentum unloading as well as the end-of-life disposal (controlled reentry). The system consists of four pods located 90 deg apart around the bus. Each pod contains two axial MR-107K engines and two lateral MR-111C thrusters. The MR-107 K engines are responsible for deorbiting the spacecraft, while the MR-111C engines are used to unload the angular momentum of the reaction wheels. A supporting feed system was compiled using available flight-proven components. Other assumptions include a propellant residual of 3% and an ullage of 5%. The mass and component list for this notional system is shown in table 23. The table shows the dry mass components of the propulsion system, which total to 106 kg. A total of 353 kg propellant is loaded into the four tanks. In order to fill the tanks, 28.5 kg of extra maneuver propellant is included. This may help with additional momentum unloading required for the LEO environment. The total propulsion system wet mass of 462 kg includes 3.4 kg of gaseous nitrogen pressurant.

Table 23. Propulsion system MEL for LEO configuration.

Item	Quantity	Unit Mass (kg)	Basic Mass (kg)	Contingency		Predicted Mass (kg)	Information
				(%)	(kg)		
Propulsion total			81.45	30	24.43	105.88	
Axial thrusters	8	0.91	7.28	30	2.18	9.46	Aerojet MR-107K
Lateral thrusters	8	0.33	2.64	30	0.79	3.43	Aerojet MR-111C
Propellant tanks	4	13.15	52.61	30	15.78	68.39	ATK (80469-1)
Pressurant fill/ drain valve	4	0.21	0.84	30	0.25	1.09	Moog (50E889)
Pressure transducers	8	0.28	2.24	30	0.67	2.91	Lunar Prospector
Temperature sensors	20	0.1	2.08	30	0.62	2.7	FCI (AS-TT)
Propellant filters	4	0.3	1.2	30	0.36	1.56	VACCO (F1D10559-01)
Flow control orifice	4	0.02	0.08	30	0.02	0.1	AIAA 2003-4470
Latch valves	7	0.5	3.5	30	1.05	4.55	Moog (51-134)
Propellant fill/ drain valves	4	0.21	0.84	30	0.25	1.09	Moog (50-856)
Lines and fittings	1	2.45	2.45	30	0.74	3.19	Estimate
Structural mounts	1	5.68	5.68	30	1.7	7.39	Estimate

10.5 Configuration

The additional propellant tanks and associated propulsion system components fit within the baseline spacecraft bus volume, as shown in figure 18. The team assumes that modifications to other subsystems will not have a large impact on the volume required for respective components.

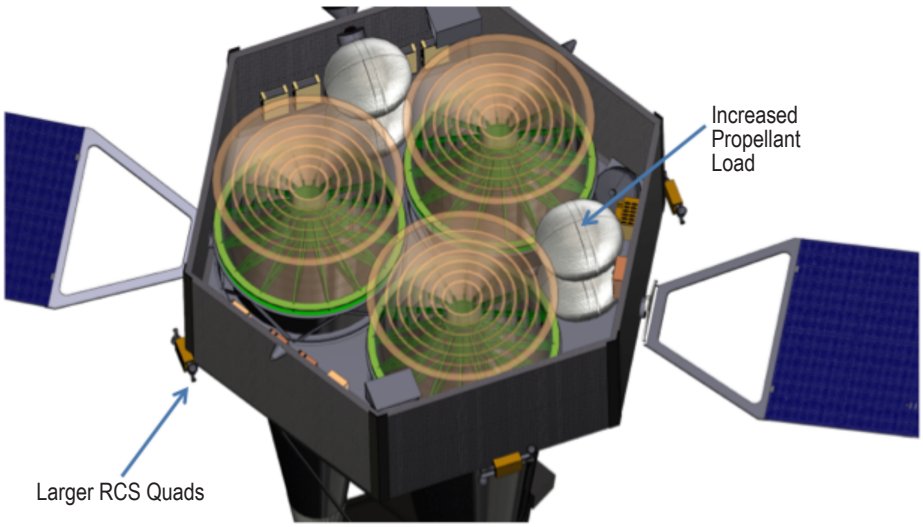

Figure 18. Notional LEO configuration showing additional propellant tanks.

10.6 All Other Subsystems

Proposed modifications to the remaining subsystems are based on engineering judgment and not analysis. Only the propulsion system was sized with the assumption that it would drive any mass change to the observatory. A brief summary of other subsystem modifications is presented below.

Even with the additional propellant, no structural modifications are required. The baseline structure is sufficient to support the additional propellant during launch. The shorter eclipse period impacts the power subsystem design slightly with a reduced energy storage requirement but a higher charge power. Mass of the secondary batteries may be reduced by 60%, while solar arrays grow by 30%. Also, lighter BroadReach power electronics could be used since the spacecraft remains inside the Van Allen belts during its mission. Since the LEO environment is typically warmer, equipment interface temperatures may increase, but this will probably result in only minor changes to the thermal control system. One important area to be considered, however, is the temperature of the CCD assembly. The assembly radiator may require repositioning or shielding to achieve the desired CCD temperature of –90 °C. The communication system will probably be affected by an LEO orbit. The Near Earth Network can be used instead of DSN. Multiple station access would be required to get 60 min of link time per day. However, there is probably not much difference in mass between the systems. A reduction in required transmission power is possible, saving about 20 W. Existing reaction wheels should work in LEO also, which are capable of 60 deg slews in 5 min for Sun avoidance, for example. Magnetic torque rods can be utilized in LEO. This would reduce RCS propellant needs for reaction wheel momentum dumping. Torque rods are preferred for momentum dumping in LEO since the system is not resource limited. Dedicated momentum dumping thrusters would not be required. However, there would probably not be much in overall mass savings. The addition of torque rods, electronics, and power required nullify propellant savings.

In summary, the design team found no reason why the current bus design could not operate in LEO with minor modifications, even though the thermal considerations regarding the CCD should be investigated. The Falcon 9 launch vehicle has plenty of mass margin for placing the observatory into the desired orbit, even when accounting for a 15% performance reserve.

11. CONCLUSIONS

In summary, the conceptual design study resulted in a spacecraft design that meets all requirements and requires no new technologies. With an estimated launch mass of just over 2,800 kg, the observatory should easily fit on an Atlas V 521, which has a capacity of 3,305 kg to the target Chandra-type orbit. Deducting a 15% launch vehicle reserve, the vehicle can still deliver 2,805 kg, which is sufficient to launch WFXT. Table 24 provides a brief summary of the design study results.

Table 24. Brief summary of spacecraft design.

Quick Summary	
Observatory mass (kg)	2,625
Launch mass (kg)	2,806
Launch vehicle	Atlas V 521
Maximum payload (kg) (with 15% margin)	3,305 (2,805)
Technologies requiring development	None

The design team also concluded that modifications to the spacecraft for operating in LEO should be minor. However, the science instrument designers would need to analyze the instrument performance, as the LEO thermal environment is very different from the baseline Chandra-type orbit.

REFERENCES

1. Murray, S.S.; Vikhlinin, A.; Forman, W.; et al.: "Wide Field X-Ray Telescope Mission," in response to RFI NNH11ZDA018L, *Wide Field X-ray Telescope*, 2011, Johns Hopkins University, <wfxt.pha.jhu.edu/docs/WFXT_RFI.pdf>.

2. Murray, S.S.; Norman, C.; Ptak, A.; et al: "Wide Field X-Ray Telescope Mission," in *Proc. SPIE*, Space Telescopes and Instrumentation 2008: Ultraviolet to Gamma Ray, Marseille, France, June 23–28, 2008, Vol. 7011, 16 pp., doi:10.1117/12.789122, August 2008.

3. *New Worlds*, *New Horizons in Astronomy and Astrophysics*, The National Academies Press, Washington, DC, 324 pp., 2010.

4. Hopkins, R.C.; Johnson, L.; Thomas, H.D.; et al.: "Advanced X-Ray Timing Array Mission: Conceptual Spacecraft Design Study," NASA/TM—2011–216476, Marshall Space Flight Center, AL, 54 pp., November 2011.

5. Structural Design and Test Factors of Safety for Spaceflight Hardware, NASA-STD-5001A, August 5, 2008.

6. Mankins, J.C.: "Technology Readiness Levels," *NASA Headquarters*, April 6, 1995, Office of Space Access and Technology, <www.hq.nasa.gov/office/codeq/trl/trl.pdf>.

7. Manufacturing Readiness Level (MRL) Deskbook, OSD Manufacturing Technology Program, version 2.0, 81 pp., May 2011.

8. Mankins, J.C.: "Research and Development Degree of Difficulty ($R\&D^3$)," *NASA Headquarters*, March 10, 1998, Office of Space Flight, <www.hq.nasa.gov/office/codeq/trl/r&d3.pdf>.

9. Bautz, M.W.; Foster, R.F.; and Murray, S.S.: "Focal plane instrumentation for the Wide-Field X-ray Telescope," in *Proc. SPIE*, Space Telescopes and Instrumentation 2010: Ultraviolet to Gamma Ray, June 28–July 2, 2010, San Diego, CA, M. Arnaud, S.S. Murray, and T. Takahashi (eds.), Vol. 7732, 6 pp., doi:10.1117/12.857803, July 2010.

10. de Chambure, D.; Lainé, R.; van Katwijk, K.; and Kletzkine, P.: "XMM's X-ray Telescopes," ESA Directorate for Scientific Programmes, No. 100, Noordwijk, The Netherlands, 13 pp., December 1999.

11. Zhang, W.W.; Chan, K.; McClelland, R.S.; et al.: "Next Generation X-ray Optics: High-resolution, Light-weight, and Low-cost," in response to RFI NNH11ZDA018L, *Physics of the Cosmos*, 2011, Goddard Space Flight Center, <pcos.gsfc.nasa.gov/studies/rfi/Zhang-William-RFI.pdf>.

12. Bookbinder, J.: "AXSIO: The Advanced X-ray Spectroscopic Imaging Observatory," in response to RFI NNH11ZDA018L, *Physics of the Cosmos*, 2011, Goddard Space Flight Center, <pcos.gsfc.nasa.gov/studies/rfi/Bookbinder-Jay-RFI-NNH11ZDA018L.pdf>.

REPORT DOCUMENTATION PAGE

Form Approved
OMB No. 0704-0188

1. REPORT DATE *(DD-MM-YYYY)*	2. REPORT TYPE	3. DATES COVERED *(From - To)*
01–03–2014	Technical Memorandum	

4. TITLE AND SUBTITLE

Wide Field X-Ray Telescope Mission Concept Study Results

5a. CONTRACT NUMBER

5b. GRANT NUMBER

5c. PROGRAM ELEMENT NUMBER

6. AUTHOR(S)

R.C. Hopkins, H.D. Thomas, L.L. Fabisinski,* M. Baysinger,**
L.S. Hornsby,** C.D. Maples,** T.E. Purlee,** P.D. Capizzo,***
and T.K. Percy†

5d. PROJECT NUMBER

5e. TASK NUMBER

5f. WORK UNIT NUMBER

7. PERFORMING ORGANIZATION NAME(S) AND ADDRESS(ES)

George C. Marshall Space Flight Center
Huntsville, AL 35812

8. PERFORMING ORGANIZATION REPORT NUMBER

M–1380

9. SPONSORING/MONITORING AGENCY NAME(S) AND ADDRESS(ES)

National Aeronautics and Space Administration
Washington, DC 20546–0001

10. SPONSORING/MONITOR'S ACRONYM(S)

NASA

11. SPONSORING/MONITORING REPORT NUMBER

NASA/TM—2014–218191

12. DISTRIBUTION/AVAILABILITY STATEMENT

Unclassified-Unlimited
Subject Category 18
Availability: NASA STI Information Desk (757–864–9658)

13. SUPPLEMENTARY NOTES

Prepared by the Advanced Concepts Office, Engineering Directorate
*ISSI, **Jacobs ESSSA Group, *** Raytheon, †SAIC

14. ABSTRACT

The Wide Field X-Ray Telescope (WFXT) is an astrophysics mission concept for detecting and studying extra-galactic x-ray sources, including active galactic nuclei and clusters of galaxies, in an effort to further understand cosmic evolution and structure. This Technical Memorandum details the results of a mission concept study completed by the Advanced Concepts Office at NASA Marshall Space Flight Center in 2012. The design team analyzed the mission and instrument requirements, and designed a spacecraft that enables the WFXT mission while using high heritage components. Design work included selecting components and sizing subsystems for power, avionics, guidance, navigation and control, propulsion, structures, command and data handling, communications, and thermal control.

15. SUBJECT TERMS

x-ray astrophysics, active galactic nuclei, spacecraft design

16. SECURITY CLASSIFICATION OF:			17. LIMITATION OF ABSTRACT	18. NUMBER OF PAGES	19a. NAME OF RESPONSIBLE PERSON
a. REPORT	b. ABSTRACT	c. THIS PAGE			STI Help Desk at email: help@sti.nasa.gov
U	U	U	UU	60	19b. TELEPHONE NUMBER *(Include area code)* STI Help Desk at: 757–864–9658

National Aeronautics and
Space Administration
IS20
George C. Marshall Space Flight Center
Huntsville, Alabama 35812